Int J Earth Sci (Geol Rundsch) (2015) 104:1039–1060
DOI 10.1007/s00531-014-1130-6

ORIGINAL PAPER

Accretionary prism–forearc interactions as reflected in the sedimentary fill of southern Thrace Basin (Lemnos Island, NE Greece)

A. G. Maravelis · G. Pantopoulos · P. Tserolas · A. Zelilidis

Received: 23 March 2014 / Accepted: 12 December 2014 / Published online: 25 December 2014

Abstract Architecture of the well-exposed ancient forearc basin successions of northeast Aegean Sea, Greece, provides useful insights into the interplay between arc magmatism, accretionary prism exhumation, and sedimentary deposition in forearc basins. The upper Eocene–lower Oligocene basin fill of the southern Thrace forearc basin reflects the active influence of the uplifted accretionary prism. Deep-marine sediments predominate the basin fill that eventually shoals upwards into shallow-marine sediments. This trend is related to tectonically driven uplift and compression. Field, stratigraphic, sedimentological, petrographic, geochemical, and provenance data on the lower Oligocene shallow-marine deposits revealed the accretionary prism (i.e. Pindic Cordillera or Biga Peninsula) as the major contributor of sediments into the forearc region. Field investigations in these shallow-marine deposits revealed the occurrence of conglomerates with: (1) mafic and ultramafic igneous rock clasts, (2) low-grade metamorphic rock fragments, and (3) sedimentary rocks. The absence of felsic volcanic fragments rules out influence of a felsic source rock. Geochemical analysis indicates that the studied rocks were accumulated in an active tectonic setting with a sediment source of mainly mafic composition, and palaeodispersal analysis revealed a NE-NNE palaeocurrent trend, towards the Rhodopian magmatic arc. Thus, these combined provenance results make the accretionary prism the most suitable candidate for the detritus forming these shallow-marine deposits.

Keywords Oligocene · Provenance · Accretionary prism · Forearc setting · Thrace Basin

A. G. Maravelis (✉)
School of Environmental and Life Sciences,
University of Newcastle, Callaghan, NSW 2308, Australia
e-mail: Angelos.Maravelis@newcastle.edu.au

G. Pantopoulos
Instituto de Geociências, Universidade Federal do Rio Grande do Sul (UFRGS), Campus do Vale Av. Bento Gonçalves 9500, Porto Alegre CEP 91501-970, Brazil

P. Tserolas · A. Zelilidis
Laboratory of Sedimentology, Department of Geology, University of Patras, Patras, Greece

Introduction

Active convergent margins are recognized as the primary locations at which crust is both created and recycled back to the mantle (e.g. Clift et al. 2005; Fildani et al. 2008; Kochelek et al. 2011). Forearc basins, sited on the oceanward edge of actively deforming convergent margins, may contain an excellent record of the tectonic evolution of these dynamic plate boundaries (e.g. Dickinson and Seely 1979; Ingersoll 1983; Unruh et al. 2007; Trop 2008; Mitchell et al. 2010; Maravelis and Zelilidis 2013). Forearc basins constitute major sites of sediment accumulation located between the subduction complex and the magmatic arc, and they evolve in response to (1) tectonic forcing related to subduction processes, (2) eustatic changes in sea level and their effects on the depositional profile, (3) isostatic subsidence due to forearc sediment loading, which in turn is related to tectonic, climatic, and eustatic controls, and (4) flat-slab subduction of spreading ridges and thick oceanic crust (DeGraaff-Surpless et al. 2002; Clift et al. 2005; Fildani et al. 2008; Finzel et al. 2011; Paquet et al. 2011; Ridgway et al. 2012; Kortyna et al. 2013; Maravelis and Zelilidis 2013). Ancient forearc basins can be examined in outcrop in some instances (e.g. Clift et al. 2005; Maravelis et al. 2007; Fildani et al.

2008; Trop 2008; Wang et al. 2012), but typically are significantly altered by collisional tectonics and may be lost altogether because of underthrusting or uplift and erosion. Seismic data can add useful constrains into our understanding of the stratigraphic architecture of forearc basin fills (Laursen and Normark 2003; Berglar et al. 2008; Williams and Graham 2013) and can also provide information for basin-scale correlations, but their use in establishment of depositional environments is limited (Marcaillou and Collot 2008). Thus, the drivers of sediment accumulation and stratigraphic packaging in forearc basins are less well known than for basins in extensional or foreland settings (Mitchell et al. 2010). Sedimentary records of ancient forearc basins can provide a more complete history of arc magmatism and topography. Provenance analysis of forearc strata is also important because it can elucidate many arc–forearc region characteristics such as palaeotopography of the arc, regional drainage patterns between the arc and forearc basin, and the magmatic history of the arc (DeGraaff-Surpless et al. 2002).

Cenozoic rocks in the eastern Balkan Peninsula form one of the best-exposed active continental margin basin complexes in the world (Turgut et al. 1991; Turgut and Eseller 2000). The Thrace Basin extends across the Hellenic, Bulgarian, and Turkish domains (D'Atri et al. 2012; Maravelis and Zelilidis 2013) and contains a record of forearc–arc evolution fundamental to understanding the Paleogene convergent margin of African–Eurasian plate boundary (Fig. 1). The basin has been considered as a forearc basin of the "contracted" type (Görür and Okay 1996; Maravelis and Zelilidis 2010) and is the largest and thickest Tertiary sedimentary basin of the eastern Balkan region (Turgut et al. 1991; Turgut and Eseller 2000). A large accretionary prism in the central Aegean region (outcropping at Biga Peninsula of NW Turkey) bounds the basin on the seaward side, and the landward flank was

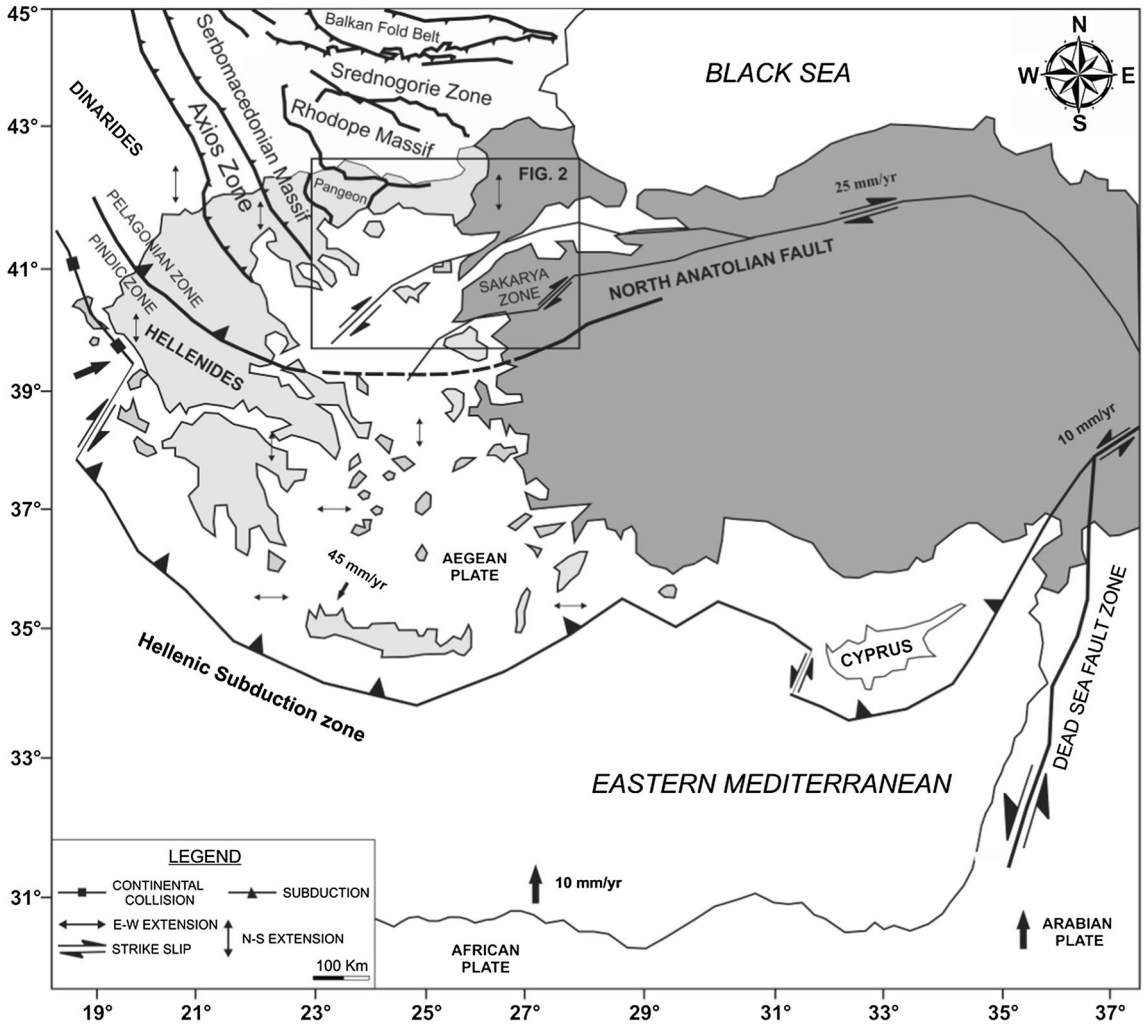

Fig. 1 Map depicting the plate tectonic configuration of the eastern Balkan Peninsula and the position of the study area in relation to the main Alpine orogenic elements of the region (from Dimitriadis et al. 1998; Maravelis and Zelilidis 2013; Tranos and Lacombe 2014)

bound by an active volcanic arc, the Rhodopian arc. Most of the basin strata are Lower Eocene to Upper Oligocene and form thick sedimentary successions (up to 9,000 m) consisting mostly of sand-rich deep-sea fan deposits (Turgut et al. 1991; Turgut and Eseller 2000). Previous studies have documented that the Hellenic part of the Thrace Basin was mainly influenced by two major sediment inputs (Maravelis and Zelilidis 2010, 2013). The southern (accretionary) part of the basin (Lemnos Island) was affected by the accretionary prism and associated ophiolitic units (Maravelis and Zelilidis 2010, 2013), while the northern (arcwards) part (Rhodope area) reflects a Rhodopian magmatic arc influence (Maravelis and Zelilidis 2010; Caracciolo et al. 2011). The present study provides additional insights into the provenance, palaeodispersal pattern, and sediment source nature of this complex two-sided forearc basin using new fieldwork and geochemical data.

More particularly, this research employs: (1) sedimentological data to provide a comprehensive overview of the sedimentary facies, allowing the depositional processes and environments to be characterized, (2) palaeocurrent data to reveal the palaeoflow direction, (3) conglomerate clast composition data, and, (4) major- and trace-element provenance data to identify the source rock compositions. Based on the obtained results, it is suggested that Paleogene sediments in the Hellenic southern part of the Thrace Basin are affected by the active influence of the accretionary prism rather than the erosion of the Rhodopian arc. Consequently, the present study is also useful in documenting a basin example which can serve as a reference for future analysis of similar two-sided forearc basin successions characterized by significant sediment input from a trenchward prism.

Geologic setting

The Thrace Basin was formed as an elongate trough between the Rhodopian magmatic arc to the north and the accretionary prism (Pindic Cordillera in Greece and Biga Peninsula in Turkey) to the south (Görür and Okay 1996; Tranos 2009; Maravelis and Zelilidis 2010; D'Atri et al. 2012; Maravelis and Zelilidis 2013). This prism is considered to represent the westward continuation of the Intra-Pontide or the more southern İzmir-Ankara oceans which are related to the closure of the Neo-Tethyan oceanic basin (Okay et al. 2008). The sedimentary rocks of the Thrace forearc basin overlie the rocks of the Rhodope magmatic arc to the north and the southern basin fill is underlain by ophiolitic and metamorphic rocks, which form part of the accretionary prism (Elmas 2012). This sedimentary fill, and particularly the sediments located at the southern Hellenic part of the basin, can provide insights for the regional geodynamic evolution.

The southern flank of the basin is deformed by the North Anatolian Fault (NAF). Estimated ages for the initiation of motion along the NAF range from the late Miocene to late Pliocene, and thus, it was not active during deposition (Dewey and Sengör 1979; Topuz et al. 2008). The NAF total displacement has been estimated using large river valleys and structural markers that indicate a Neogene slip rate of 6.5 mm/yr over 13 Myr (Hubert-Ferrari et al. 2002). A large part of the Thrace Basin is located in the North Aegean Trough (NAT) that constitutes the modern basin established over the Tertiary Thrace Basin (Tranos 2009). The NAT is a ~300-km-long narrow trough in the North Aegean Sea and is located along the Tethyan Ocean (Axios zone in Greece and Intra-Pontide suture zone in Turkey) (Mountrakis 2006) (Fig. 2). Structural analysis suggests that the formation and widening of the NAT were not related to the propagation of the NAF into the North Aegean Sea, but to the late collisional processes between Apulia and Eurasia plates during the late Oligocene–middle Miocene time (Tranos 2009).

The Hellenic continental margin, which results from the oblique subduction of the oceanic African Plate beneath Eurasia, has played a key role in controlling magmatism in the Balkan Peninsula since late Cretaceous (Fytikas et al. 1984; Marchev et al. 2004; Bonev and Beccaletto 2007). A subduction mechanism has been proposed to explain late Cretaceous magmatism in southern Bulgaria, with the Rhodope being considered as the frontal part of Srednogorie arc (Marchev et al. 2004). A southward magmatic migration from 92 to 78 Ma is evidenced by U–Pb zircon dating (Peytcheva et al. 1998). The occurrence of Srednogorie zone into the southern Rhodope region is documented by the 70–42 Ma granitoid intrusions. Lower Miocene volcanic rocks are common in the North Aegean Sea, indicating further southward migration (Innocenti et al. 1994; Yilmaz et al. 2001; Maravelis et al. 2007). An extended subduction event has been invoked to account for the continuous regional magmatism (Marchev et al. 2004). The magmatic activity commenced in Rhodope in late Eocene and its migration suggests that the present day northward subduction in the Aegean region initiated during Eocene time (Fytikas et al. 1984; Spakman et al. 1988).

At the subduction zone, the accretion of oceanic crust and sediment to the upper plate caused the growth of an accretionary prism (Maravelis and Zelilidis 2010, 2013; D'Atri et al. 2012; Görür and Elbek 2013). The occurrence of eclogites and blueschists in the accretionary prism area (Biga Peninsula) suggests eclogite/blueschist-grade metamorphism (Topuz et al. 2008; Şengün et al. 2011). This metamorphic event along with the presence of an ophiolitic mélange has been ascribed to Tertiary subduction processes that led to the formation of the Hellenic orogen (Beccaletto et al. 2005; Okay et al. 2010; Maravelis and Zelilidis 2010,

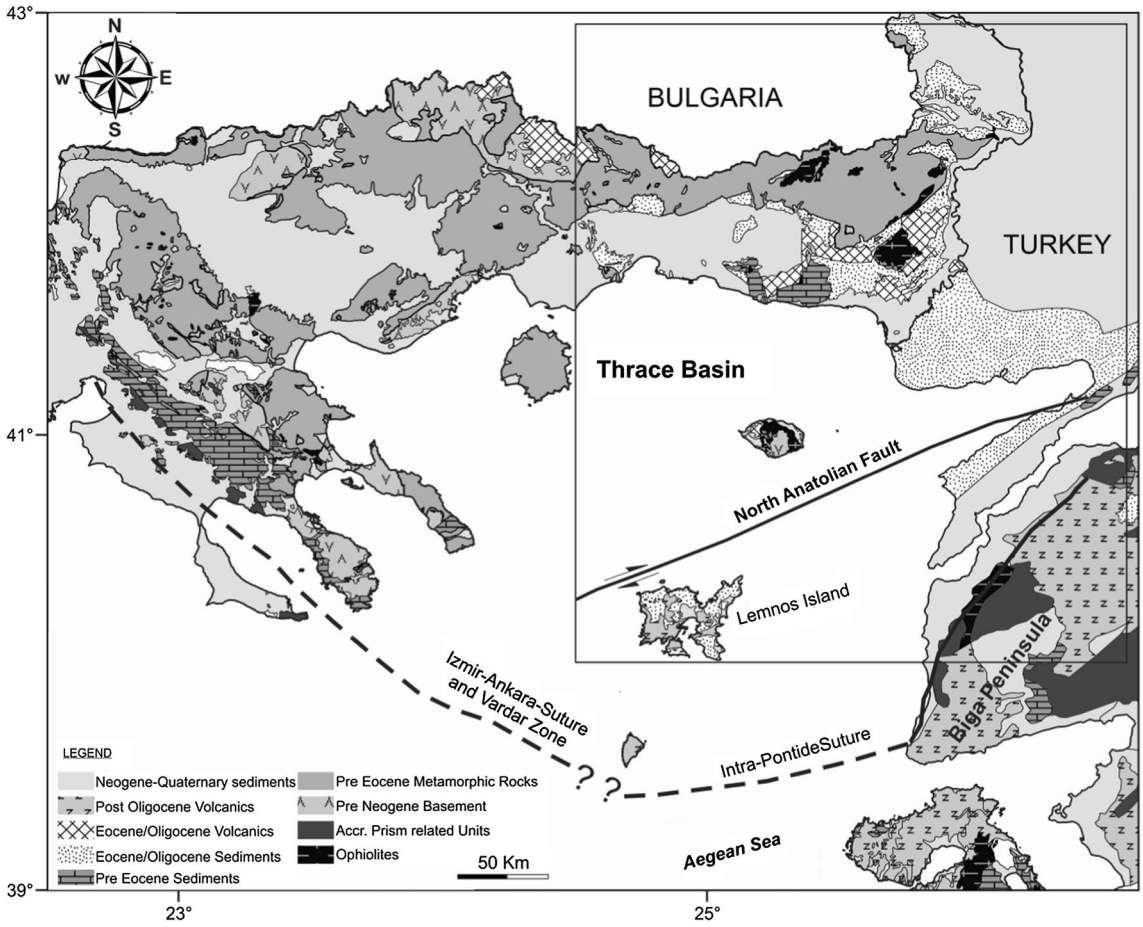

Fig. 2 Geologic sketch map of the Thrace Basin showing the pre-Eocene basement, the Eocene to Oligocene sediment, the post-Eocene deposits, and the volcanic domains (from Bonev and Beccaletto 2007)

2013). Between the Rhodopian magmatic arc and the accretionary prism, sediment filling the Thrace forearc basin comprises the Eocene to Oligocene clastic strata (Turgut et al. 1991; Turgut and Eseller 2000; Maravelis et al. 2007; Maravelis and Zelilidis 2011). Provenance analyses utilizing sandstone petrography, conglomerate clast composition and bulk-rock geochemistry indicate that the basin is two-sided (Maravelis et al. 2007; Maravelis and Zelilidis 2010; D'Atri et al. 2012).

Sedimentation along the arcward basin margin was dominated by deposition of carbonates during the Eocene and by deltaic bodies, prograding towards the basin centre, in the Oligocene (Turgut et al. 1991). The seaward part of the Thrace Basin is dominated by a sand-rich submarine-fan system that underlies slope and shallow-marine deposits; palaeoflow data indicate northeastward sediment transport (Perinçek 1991; Turgut et al. 1991; Maravelis et al. 2007; Maravelis 2009; Maravelis and Zelilidis 2011). The source area contributed a significant volume of ultramafic, gabbro, basalt, chert, and possibly some volcaniclastic detritus of variable grain size into the forearc basin (Görür and Okay 1996; Maravelis and Zelilidis 2010; D'Atri et al. 2012). The source area was probably rapidly eroded, causing the ophiolitic bedrock to be deeply incised and enabling a significant amount of coarse-grained material to be transported to the forearc region (Görür and Okay 1996; Maravelis and Zelilidis 2010; D'Atri et al. 2012). In the landward parts of the basin (Rhodope region), shelves fringed the Rhodopian arc and fed abundant coarse-grained sediment down the slope to the deep portions of the forearc basin. This sediment formed extensive submarine-fan deposits that crop out along the northern flank of the forearc basin (Maravelis and Zelilidis 2010, 2013).

During the Miocene, Thrace Basin was the site of volcanic activity resulting in accumulation of magmatic rocks, principally trachyandesites and dacites (Pe-Piper and Piper 2001). These rocks have been interpreted as belonging to the northern, "shoshonitic province" along the Aegean–Anatolian boundary that includes the islands of Samothrace, Lemnos, and Lesvos (Pe-Piper et al. 2009). These high-K rocks, mostly of intermediate composition, indicate ensuing calc-alkaline orogenic volcanism, emitted from

large volcanic centres. Upwelling of asthenospheric mantle has been invoked to account for their genesis (Pe-Piper et al. 2009).

Basin stratigraphy, architecture, and evolution

The late Eocene to early Oligocene sand-rich submarine-fan systems in southern Thrace Basin (Lemnos Island and Biga Peninsula) have been extensively described and indicate an active tectonic setting (Perinçek 1991; Roussos 1994; Maravelis 2009; Maravelis and Zelilidis 2011). In Lemnos Island, this system has been subdivided into a basal outer and an overlying inner fan shape (Figs. 3, 4). The outer fan is equivalent to the low-stand fan and is composed of lobe, lobe-fringe, and fan-fringe deposits. The inner fan is equivalent to the low-stand wedge and is further subdivided into a channel-fill and levee system that evolves upwards into a conglomeratic channel-fill system. This submarine-fan system occurs as a laterally isolated body, with a single sediment source consisting of a proximal distributary channel. This source occupies a position approximately in the centre of the fan and contains the coarsest sediment in the study area. This stratigraphic architecture, in conjunction with the north-northeastward palaeoflow direction, indicates a curved fan shape.

The sequence stratigraphic framework was constructed by observing changes in depositional setting, facies, and types of gravity-flow deposits with time (Catuneanu et al. 2011; De Gasperi and Catuneanu 2014). The base of the

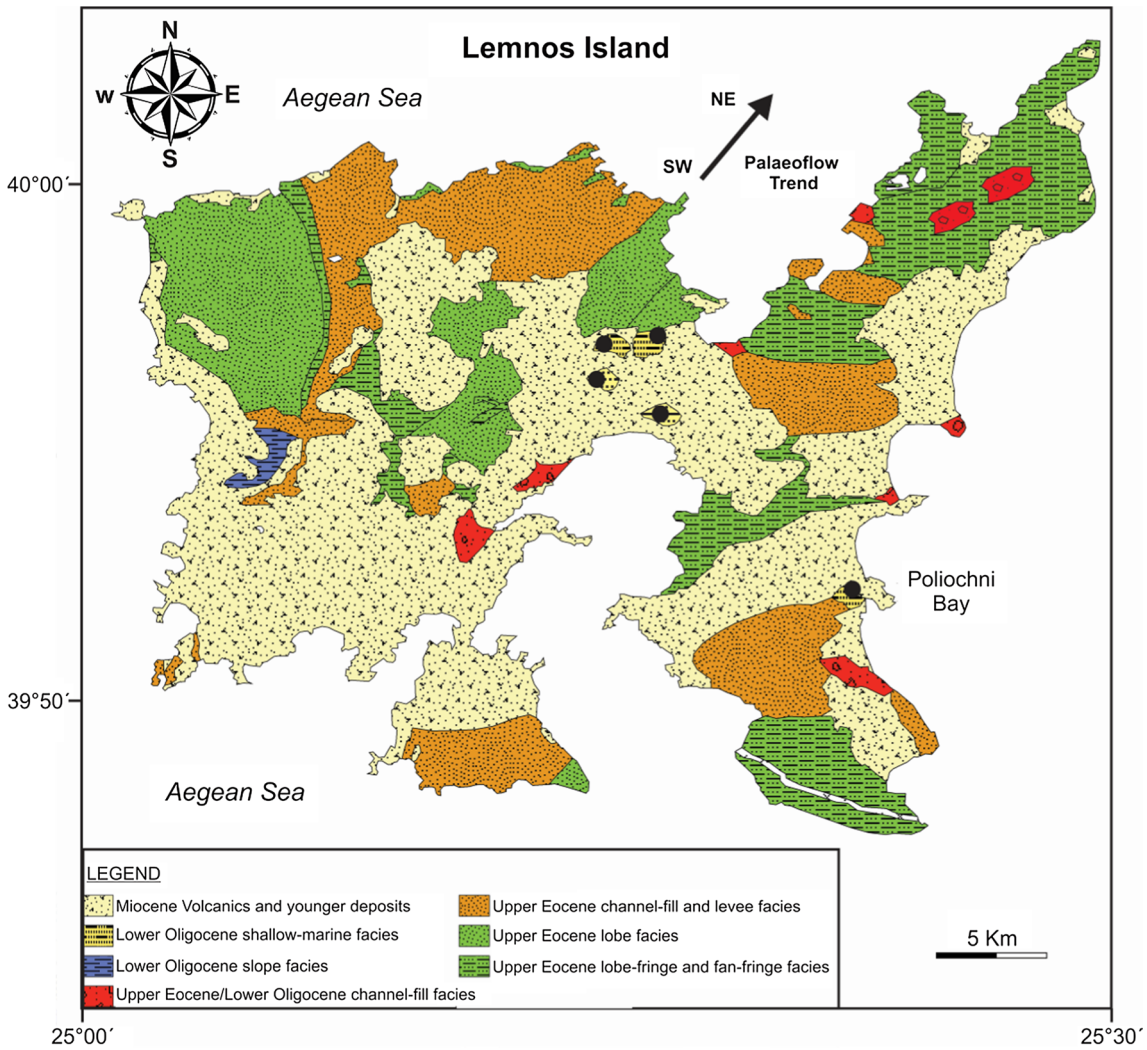

Fig. 3 Detailed geologic map of the southern margin of the Hellenic Thrace Basin (Lemnos Island) where upper Eocene to lower Oligocene submarine fans evolve up-sequence into lower Oligocene slope and swallow-marine facies (Roussos 1994; Maravelis and Zelilidis 2012). Note the seven different recognized sub-environments. The *black arrow marks* the main palaeoflow direction and the *black dots* correspond to the sample locations (from Maravelis et al. 2007; Maravelis and Zelilidis 2011)

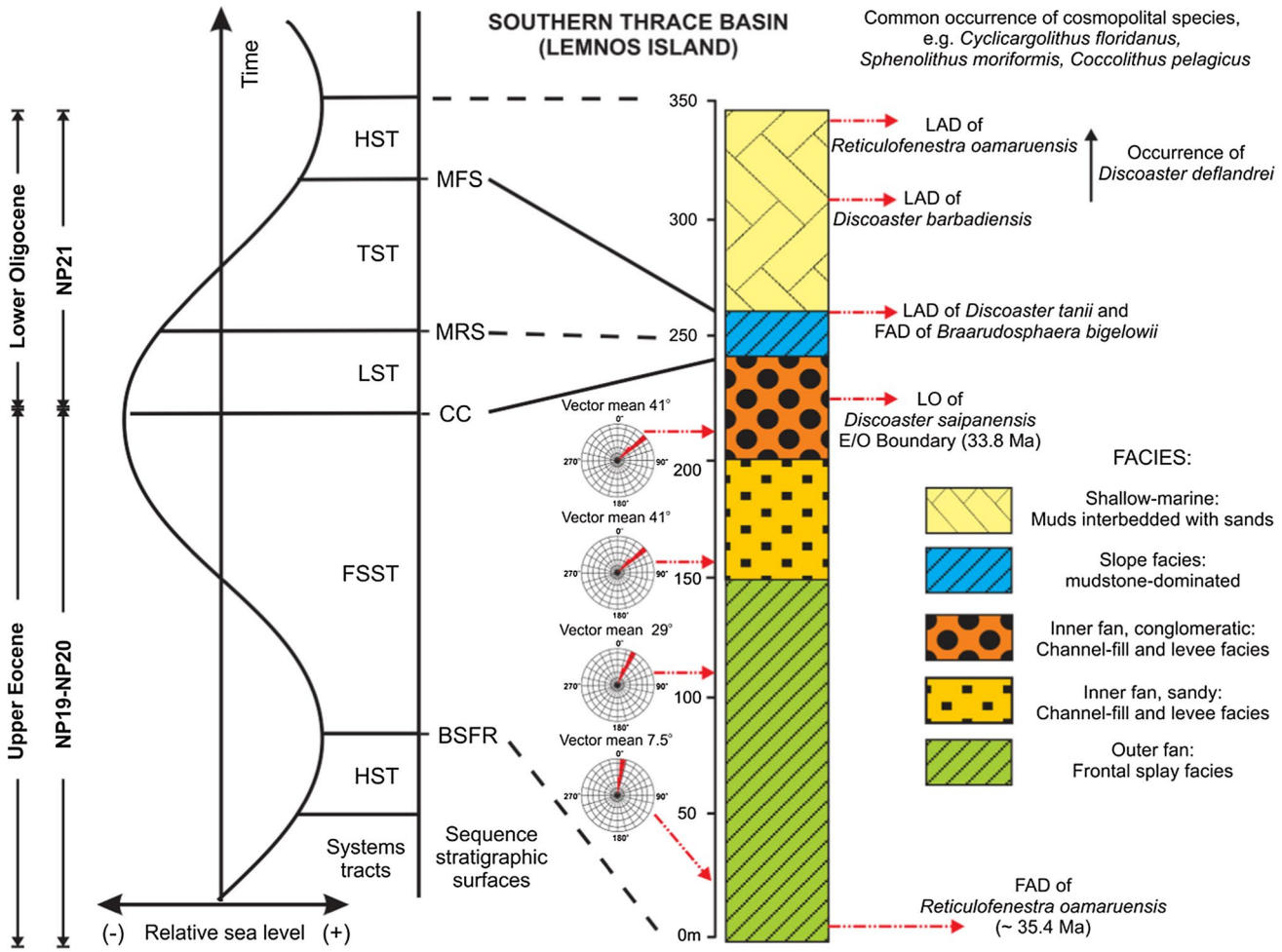

Fig. 4 Calcareous nannofossil biostratigraphic zonation and sequence stratigraphic framework for the Upper Eocene to Lower Oligocene depositional sequence of Lemnos Island. Note the NE palaeoflow direction of the underlying submarine fans (from Roussos 1994; Maravelis et al. 2007). Note the long-term (second order) progradational trend from the basin-floor fan to the shallow-marine deposits and the interpretation of the depositional facies in terms of third-order systems tracts (from Maravelis and Zelilidis 2012). FSST: falling-stage system tract; HST: highstand system tract; LST: low-stand system tract; BSFR: basal surface of forced regression; CC: correlative conformity; MRS: maximum regressive surface; MFS: maximum flooding surface; FAD: first appearance datum; FO: first occurrence; LAD: last appearance datum

submarine-fan system in the southern part of the Thrace Basin is not exposed, and therefore, the basal surface of forced regression (BSFR) is not observed in outcrop in this case study. The correlative conformity (CC) that forms at the end of forced regression is one of the most prominent sequence stratigraphic surfaces in the deep-water setting, as it marks the end of high sediment supply to the deep-water environment, and consequently an abrupt shift to finer grained sediment. This surface is exposed within our study area, at the top of the conglomeratic fan system (Fig. 4). The maximum regressive surface (MRS), which forms during relative sea-level rise, is typically cryptic in the deep-water setting as there is no marked change in sediment supply from low-stand normal regression to transgression (Catuneanu et al. 2009). The MRS may be placed anywhere within the mudstone-dominated slope facies that overlie the conglomeratic fan system (Fig. 4). The maximum flooding surface (MFS), which also forms during relative sea-level rise at the time of maximum shoreline transgression on the shallow marine when sediment supply to the deep-water environment decreases to a minimum, may also be cryptic and placed within a condensed section. In our case study, the MFS is taken at the top of the mudstone-dominated slope facies (facies 4 in Fig. 4), which marks the base of the overlying coarsening-upward high-stand shallow-marine deposits (facies 5 in Fig. 4).

In summary, a sand-rich submarine-fan system along with overlying slope and shallow-marine deposits spans the Eocene/Oligocene boundary on Lemnos Island. During late Eocene (NP19/NP20), the outer fan system, the inner fan

and the lower part of the conglomeratic fan accumulated. Subsequently, the remainder of the inner fan system was deposited during the early Oligocene (NP21). Eventually, during the late parts of the early Oligocene (NP21), the up-sequence slope and shallow-marine deposits accumulated (Maravelis and Zelilidis 2012).

Materials and methods

This investigation uses data derived from outcrop-based sedimentary facies analyses to reconstruct a palaeodepositional history of the basin; palaeodispersal data to reveal the palaeocurrent direction; conglomerate composition data and inorganic geochemical analyses of mudstone in order to unravel the provenance and tectonic setting. Depositional processes, environments, and sub-environments were interpreted by using primary sedimentological features. Calcareous nannofossils were utilized to constrain palaeobathymetry, palaeoenvironment, and timing of key stratigraphic levels in the basin (Maravelis and Zelilidis 2012). Palaeodirection analysis was performed for the first time on the lower Oligocene shallow-marine facies, expanding on previously published work conducted on the underlying submarine fans (Maravelis et al. 2007). Palaeoflow data were obtained by measuring sole marks and foreset laminae. For conglomerate compositional analysis, a one-square-metre frame was used and compositions noted at 100-mm grid intersections; simple average values are reported. X-ray fluorescence (XRF) spectroscopy was used to quantify the major and trace elements of the twenty (20) selected mudstone samples. Samples collected from natural outcrops in order to be representative of the regional basin history (Figs. 3, 5). A cut of each sample is thoroughly washed in cold water. Any large quantities of contaminants, such as lost circulation material, are removed. The washed contaminants or obvious cavings are removed. The sample is then air-dried at room temperature and subsequently crushed to a homogeneous powder and bagged in readiness for analysis. XRF analysis was performed using Niton XL3t Goldd + analyser. Thermo Scientific Niton XL3t analysers are equipped with excitation filters that optimize the analysers' sensitivity for various elements. The "high-range" filter is used to optimize barium (Ba) through silver (Ag). The "main-range" filter provides optimum sensitivity for the elements manganese (Mn) through bismuth (Bi). The "low-range" filter is used to optimize the sensitivity for the elements from titanium (Ti) through chromium (Cr). The "light-range" filter is available only with He-purged and Goldd technology analysers and is used in light element analysis such as (Mg). Optimal results were obtained from powder samples with the use of a He purge system.

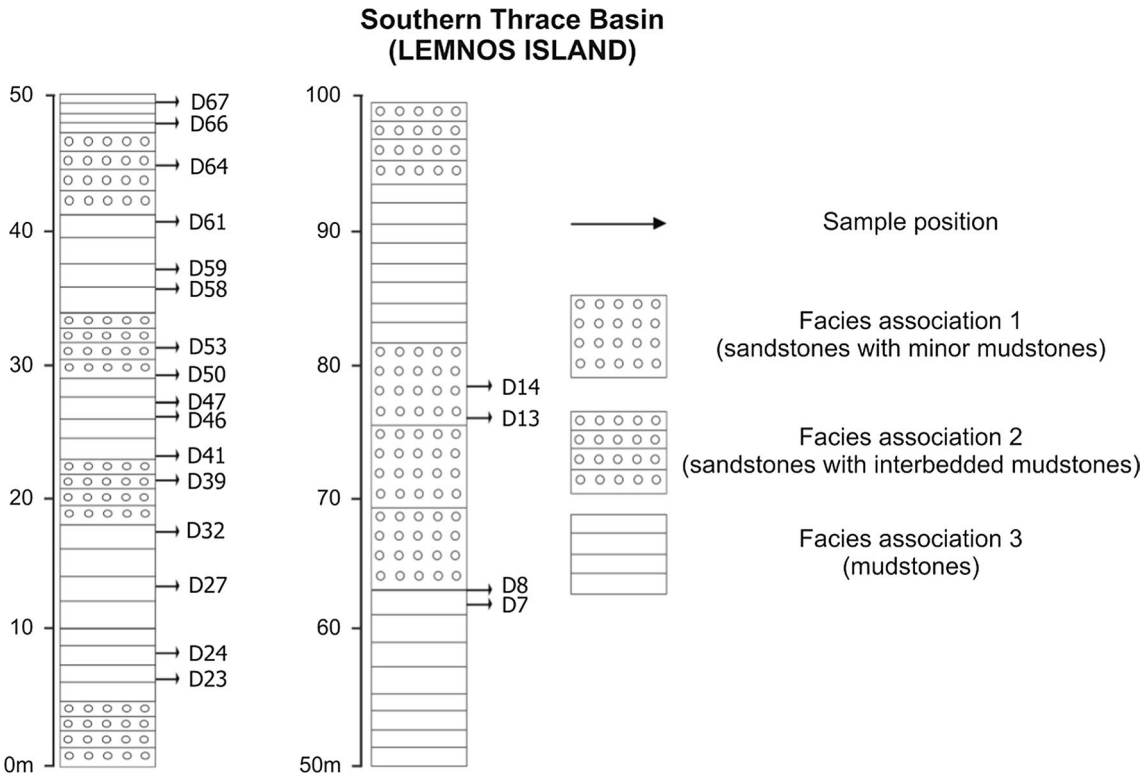

Fig. 5 Lithological (metre scale) section of the studied shallow-marine sediments showing the stratigraphic position of the examined samples

Counting times were 30 s each on the low- and high-energy filters (for analysing elements K to U), and 60 s on the main and light filter setting (Mg to S) for a total analysis time of 180 s. All the analytical process was performed in the StratoChem Laboratories, Cairo, Egypt, with the use of a Thermo Scientific Niton XRF analyser.

Facies associations

Each of the three sedimentary facies associations (FA1, FA2, and FA3; Fig. 5) described in this section is made up of a definitive set of lithofacies, which may consist of several smaller beds and bed sets with various sedimentary structures that are interpreted to have genetically related formative processes. These lithofacies sets were then grouped into a series of facies associations on the premise that several closely spaced lithofacies with similar sedimentary features and depositional processes are genetically related and have palaeoenvironmental significance (Dixon et al. 2012).

Facies association FA1: sandstone with minor mudstone

Description

This facies association consists of stacked and amalgamated sandstone (Fig. 6a). FA1 is composed of clean, normally graded or non-graded, well-sorted sandstone. Sandstone beds are characteristically sharp based and occur in thicknesses of up to 1.5–2 m forming sedimentary packages 7–10 m. They thin upward where they are interbedded with mudstone (Fig. 6b). Sandstone is light brown in colour, fine to medium grained, and thin to very thick bedded. Most of the sandstone is massive and structureless, although beds with parallel laminations and cross-lamination rarely occur (Fig. 6c). The base of the sandstone is commonly erosive into underlying mudstone (Fig. 6d). Locally derived mudstone clasts frequently line the base of the sandstone and internal erosion surfaces. Often, medium- to thick-bedded (0.5–1 m) conglomeratic units are present at the base of the amalgamated sandstone (Fig. 6e). These units

Fig. 6 Outcrop photographs of FA1. **a** Thick-bedded, amalgamated sandstone. **b** Medium- to thin-bedded sandstone interbedded with mudstone. **c** Normally graded, medium-bedded sandstone bed with parallel lamination. **d** Medium-bedded sandstone bed. Note the sharp contact between the sandy fill and the underlying mudstone. **e** Well-sorted to moderately sorted, polymictic, matrix-supported conglomerate (Poliochni Bay in Fig. 3, pen is ~15 cm long)

are composed of moderately to well-sorted, polymictic, matrix-supported conglomerates. Most conglomerates are ungraded, low to medium sphericity, and moderately to well rounded. Some of the conglomerate beds show imbrication of clasts.

Interpretation

The erosional relations with the underlying muds support erosion by unidirectional currents, incision, and sand infill by high-density flows within a channelized environment (Lowe 1982; Mulder and Alexander 2001). The mudstone rip-up clasts record erosion and sediment bypass (Bowman and Johnson 2013). The absence of bioturbation is consistent with very rapid deposition (Pemberton et al. 2002). The weakly developed cross-lamination and parallel lamination suggest that the traction currents were transitional flows that were becoming stratified and beginning to entrain material into their upper layers (Bowman and Johnson 2013). Conglomerate was deposited from traction carpets beneath high-concentration currents. Its deposition implies a high-concentration base to the flow that would have inhibited entrainment of bed material (Piper and Normark 2009). We suggest that such straight hyperpycnal channels are characteristic of the largest high-concentration flows, which may have armoured the bed and minimized later erosion by smaller fully turbulent flows.

Facies association FA2: sandstone with interbedded mudstone

Description

This facies association consists of thin- to medium-bedded, medium- to fine-grained sandstone with interbedded mudstone (Fig. 7a). Sandstone beds are characteristically flat-based, normally graded or non-graded, and well sorted (Fig. 7b). In the sandstone, the main primary sedimentary structures are parallel and current ripple cross-lamination (Fig. 7c). The mudstone comprises both homogenous,

Fig. 7 Outcrop photographs of FA2. **a** Thin- to medium-bedded sandstone interbedded with mudstone. **b** Medium- to thin-bedded sandstone. Note the flat contact between the sandy fill and the underlying mudstone. **c** Medium-bedded sandstone with parallel and cross-lamination. **d** Branched trace fossils developed in the studied shallow-marine deposits (*Thalassinoides paradoxicus*). **e** Medium-bedded sandstone with convolute lamination (Poliochni Bay in Fig. 3, pen is ~15 cm long)

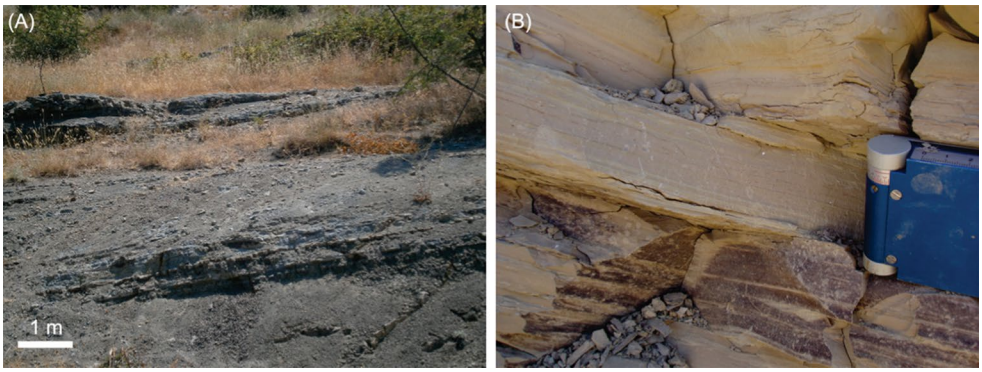

Fig. 8 Outcrop photographs of FA3. **a** Laminated mudstone with rare thin-bedded sandstone. **b** Mudstone with fine lamination (Poliochni Bay in Fig. 3)

5–50-cm-thick structureless mudstone beds and thin- to medium-bedded laminated mudstone, which contains abundant coal debris in places. FA2 forms sedimentary cycles with fining upward trends and contains trace fossils. Bioturbation is rare and where it occurs, forms low abundance, but slightly diverse assemblage, with *ophiomorpha, Thalassinoides*, and *Scolicia* (Fig. 7d). Soft-sediment deformation occurs at a variety of scales: (1) convolute bedding (tens of centimetres), (2) dish structures (1–10 cm), and (3) load structures (millimetre to centimetre scale) (Fig. 7e).

Interpretation

Homogenous, structureless mudstone beds record "frozen" cohesive muddy debris flows (Mulder and Alexander 2001). Many sandstone beds record a spectrum of depletive, waning flow processes, which resemble low-density turbidities (Kneller 1995). The various styles of sediment deformation are indicative of deposition on a relatively steep and unstable slope (Porebski and Steel 2003). Sediment load structures and convolute bedding suggest sediment liquefaction, potentially triggered by pore-pressure changes associated with seismicity, growth fault activity, mud diapirism, and storm-related wave action (Lonergan et al. 2000). Dish structures are formed by the lateral and upward passage of water through sediment (Porebski and Steel 2003).

Facies association FA3: laminated mudstone

Description

Facies association FA3 is dominated by dark blue/grey coloured mudstone with rare millimetre to centimetre-thick interbeds of laterally extensive, sharp-based sandstone. This facies association consists of thick stratigraphic units, which contain parallel laminated mudstone (Fig. 8a). Laminations are 0.1 to <2 mm thick (Fig. 8b). Individual very fine sandstone beds are non-graded and occasionally contain asymmetrical current ripple cross-lamination.

Interpretation

The mudstone is deposited from suspension under low-energy conditions. The lamination is possibly due to cyclic breaksup of flocs and turbulence damping at bed, or via bedload transport of flocs (Talling et al. 2012).

Provenance

Palaeodispersal patterns

To estimate the palaeoflow direction, palaeocurrent data from the shallow-marine sediments were measured from flute and groove marks and current ripples. Data were collected in both FA1 and FA2, although in the amalgamated sandstone strata (FA1), the only available palaeocurrent indicators were cross-lamination foresets. Several measurements were taken from each facies association (25–30), and these data are plotted in rose diagrams that document a northeastern palaeocurrent direction (Fig. 9). Palaeocurrent data are not adjusted for post-depositional rotation, but the regional 25° clockwise rotation since 17 Ma (Kondopoulou 2000) is elaborated in the discussion.

Sandstone petrography and conglomerate clast composition

Previous petrographic investigations of the submarine-fan sandstone and the overlying shallow-marine sandstone in both Hellenic and Turkish domains of the southern Thrace Basin suggest diversity of mineralogical compositions (Maravelis and Zelilidis 2010; Caracciolo et al. 2011; D'Atri et al. 2012). These studies have reached similar

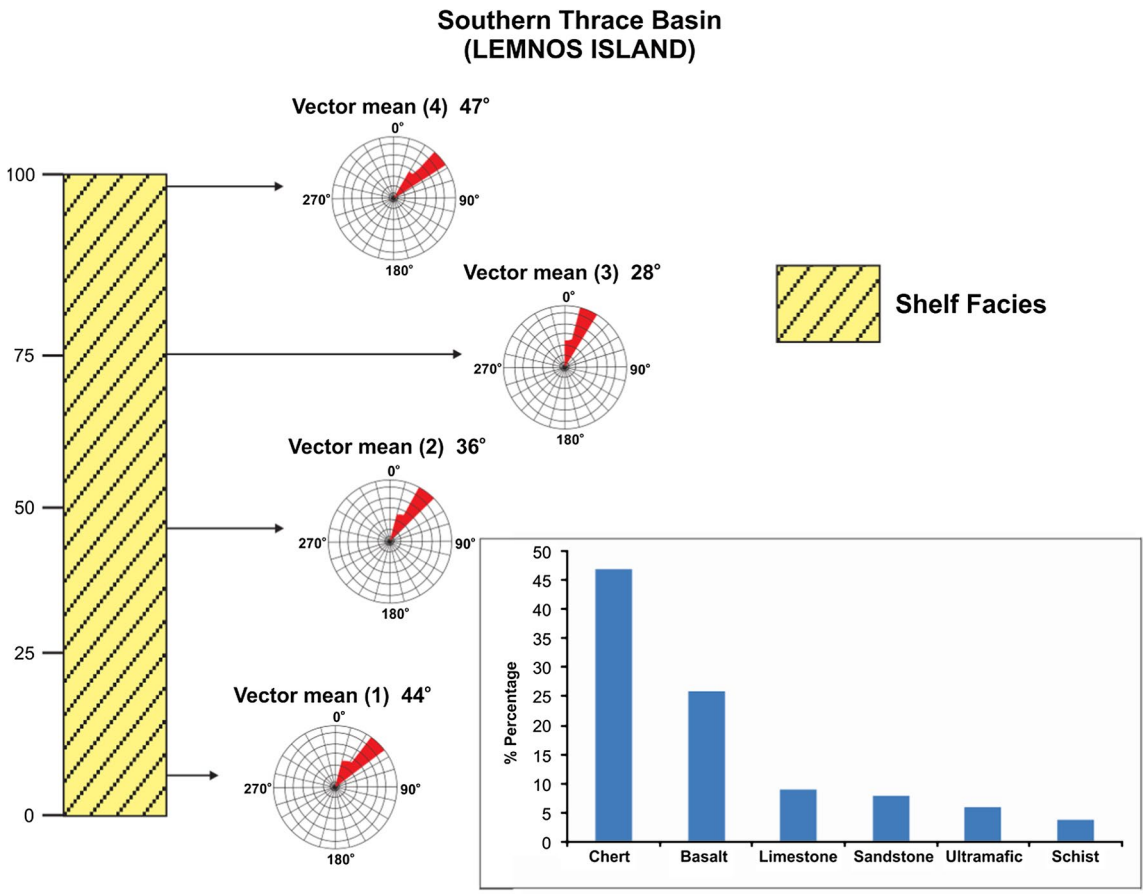

Fig. 9 Rose diagrams from the studied section showing an NE trend of the palaeocurrents' drift and conglomerate clast count results from conglomeratic units of southern Thrace Basin (Lemnos Island)

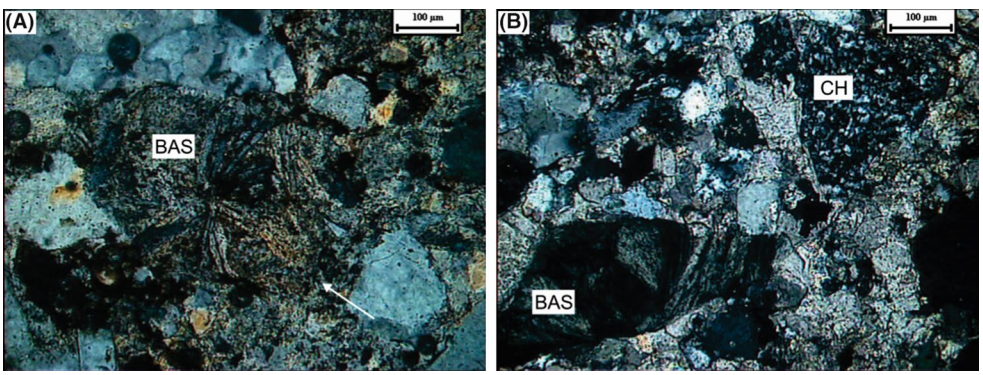

Fig. 10 Photomicrographs of lithic fragments identified within the selected sandstone samples of the southern Thrace Basin (Lemnos Island). (A) Basalt rock fragment (BAS). (B) Basalt (BAS) and Chert (CH)

conclusions, namely derivation from diverse mineralogical provinces, producing immature sandstone that is rich in lithic rock fragments. The sandstone from the southern Thrace is litharenite and wacke with abundant low-grade metamorphic rock fragments (Maravelis and Zelilidis 2010; D'Atri et al. 2012). The framework grains are mainly lithic clasts, feldspar (both K-feldspar and plagioclase), and less quartz. This sandstone is typified by the prevalence of polycrystalline quartz grains at the expense of monocrystalline quartz (Maravelis and Zelilidis 2010; D'Atri et al. 2012). Metamorphic, sedimentary, and igneous lithic fragments are abundant (Fig. 10). Metamorphic clasts consist of

schist, while sedimentary lithic fragments include those of limestone, microcrystalline chert, and sandstone. The igneous lithic fragments mainly consist of mafic basalt. Other common framework components are gabbro and peridotite rock fragments as well as glaucophane and picotite grains.

Conglomerate clasts can provide detailed provenance information, including rock type, age, bulk geochemistry, and isotopic constraints (Trop and Ridgway 2007; Fildani et al. 2008; Trop 2008; Bradshaw et al. 2012). In the study region, the conglomerate units are rare and consist of mature, moderately to well-rounded pebbles of highly resistant rock types. For compositional analysis, a one-square-metre frame was used and compositions noted at 100-mm grid intersections; simple average values are reported here (Fig. 9). Three principal rock types were distinguished within the conglomerates: (1) mafic and ultramafic igneous rocks consisting of basalt, gabbro, and peridotite, (2) low-grade metamorphic rock fragments consisting of schist, and (3) sedimentary rocks comprising sandstone, limestone, and chert. The most abundant clasts are chert (47 %) and basalt (26 %). The remaining 25 % were mainly sandstone (8 %) and limestone (9 %) as well as peridotite, gabbro, and schist (10 %). Felsic volcanic clasts were not observed.

Geochemistry

Several studies have employed major, trace, and rare earth element (REE) abundances in order to define sedimentary provenance and basin tectonic setting (e.g. Garcia et al. 1991; Nesbitt and Wilson 1992; Roser and Korsch 1986; Van de Kamp and Leake 1995; Zhang 2004; Fildani et al. 2008; Konstantopoulos and Zelilidis 2013; Tao et al. 2014). REE abundance, especially the study of the Eu anomaly in clastic sediments, is a good fingerprint for source rock characterization (Cullers 2000). Sedimentary rocks of felsic provenance exhibit negative Eu anomalies, whereas sediments with mafic influence exhibit slightly positive or no Eu anomalies (Gao and Wedepohl 1995; Cullers 2000). The study region has been influenced by a mafic source during the late Eocene to early Oligocene, as demonstrated by the geochemical and petrographic signatures of the submarine fans that underlie the lower Oligocene shallow-water sediments (Maravelis and Zelilidis 2010). Their chondrite-normalized REE patterns exhibit minor positive Eu anomalies, suggesting influx of juvenile mafic material (Maravelis and Zelilidis 2010). Here, we present the geochemistry of the overlying Oligocene shallow-marine deposits (Table 1) in order to unravel their provenance and document the presence or absence of continued mafic influence on the Oligocene section.

The contents of Cr and Ni abundance, the Cr/Ni ratio in mudstone, and the plot of Cr/V versus Y/Ni ratios are sensitive indicators of mafic–ultramafic provenance and can provide insights into determining the timing and extent of ultramafic-derived material (Hiscott 1984; McLennan et al. 1993; Garver et al. 1996; Hessler and Lowe 2006; Amorosi et al. 2007; Pantopoulos and Zelilidis 2012). The studied samples are rich in Cr and Ni, with low Y/Ni, increased Cr/V ratios, and a moderate Cr/Ni ratio (Fig. 11; Table 1). They also exhibit low Al_2O_3/TiO_2 and SiO_2/Al_2O_3 ratios as well as high Ti/Al, $100*Fe_2O_3/Al_2O_3$, and $100*TiO_2/Fe_2O_3$ ratios (Fig. 12; Table 1). The examined samples exhibit high Ti/Zr ratios and low Zr/Ni and Zr/Cr ratios (Fig. 13; Table 1). The multi-element diagrams, of Fig. 13c, display the element concentrations of the examined mudstone, normalized to the upper continental crust (UCC) composition (Taylor and McLennan 1985), on an element-by-element basis. In addition, the normalized element concentrations of sources of different compositions have been plotted for comparison. The diagram exhibits elevated abundances of V, Cr, Ni and Ti, (>1), K normalized values below unity, a marked positive CaO anomaly and also a slight positive Sr anomaly (Fig. 13c).

The geochemical results indicate mafic (and intermediate) sources, with a lack of any felsic component. This conclusion is in agreement with results from previous provenance studies of Eocene–Oligocene deep-marine sediments in the area (Maravelis and Zelilidis 2010, 2013) and is evidenced by: (a) elevated values of Cr and Ni in the studied sediments and mudstone Cr/Ni ratios of 1.3–1.5 (Garver et al. 1996; Cingolani et al. 2003), (b) the plot of Cr/V versus Y/Ni ratios, (c) relatively low Al_2O_3/TiO_2 ratios ranging below 21 (Schieber 1992; Hayashi et al. 1997), (d) high Ti/Zr ratios, much higher than those commonly recorded in felsic igneous rocks (<20) and close to the threshold of mafic igneous rocks (c. 50) according to Taylor and McLennan (1985), (e) clustering of Fe, Al, and Ti oxide discrimination diagrams around the average compositions of andesites and basalts, (f) Cr/Zr ratios well above the values seen in felsic igneous rocks (>0.5) and within the field of the mafic igneous rocks (>1), (g) SiO_2/Al_2O_3 ratios ranging close to c. 3 (Hayashi et al. 1997), (h) low Zr/Ni and Zr/Cr ratios Al, Ti, and Zr combined abundances (Garcia et al. 1991), (i) the presence of marked positive CaO and Sr anomalies in the multi-element ("spider") diagrams and similarity of UCC-normalized profiles with geochemical patterns of basaltic composition.

Discussion

Sedimentology, lithostratigraphy, sequence stratigraphy, palaeocurrent analysis, petrography, and geochemistry results suggest a forearc origin for the Thrace Basin between the Rhodopian magmatic arc in the north and the accretionary prism in the south (Pindic Cordillera and/or Biga Peninsula).

Table 1 Whole-rock major and trace element compositions of mudstone from the southern Thrace Basin (Lemnos Island). Major elements in %, trace elements in ppm

Sample	CaO	SiO_2	Al_2O_3	Fe_2O_3	TiO_2	MgO	K_2O	Ni	V	Zr	Rb	Cr	Cu	Zn
D 7	20.15	41.51	11.19	8.64	0.62	2.97	2.03	0	133	108	72	304	36	99
D 8	6.07	54.95	14.14	6.65	0.9	1.4	2.98	130	154	152	123	386	50	76
D 13	7.24	61.45	21.27	10.31	1.33	2.4	4.4	269	291	167	240	561	113	137
D 14	6.34	56.75	18.22	9.66	1.17	2.31	3.96	264	278	161	208	551	100	131
D 23	12.38	51.29	16.72	9.12	0.99	2.88	3.95	297	235	151	178	439	84	123
D 24	13.29	52.3	16.86	8.78	1.04	2.74	3.97	207	201	157	183	439	78	138
D 27	11.48	51.31	15.19	8.96	0.93	2.66	3.49	242	183	147	154	447	64	115
D 32	14.32	54.71	16.99	8.83	1.04	2.7	3.85	280	240	217	171	549	62	135
D 39	17.43	46.8	8.57	5.54	0.61	3.59	1.51	98	83	277	53	791	0	45
D 41	10.11	57.06	13.74	6.31	0.82	2.34	2.83	112	179	152	114	332	46	93
D 46	10.33	52.06	14.06	7.54	0.83	3.02	3.03	250	128	150	126	383	42	83
D 47	10.33	53.37	16.3	8.6	0.96	3.03	3.67	222	198	155	171	418	78	117
D 50	9.9	59.25	16.11	7.24	0.99	2.12	3.5	221	198	172	151	494	80	119
D 53	11.78	58.58	17.75	7.42	1.08	2.22	3.84	281	216	161	182	551	86	127
D 58	17.69	48.49	9.02	5.99	0.43	2.94	1.63	0	77	103	52	347	0	73
D 59	8.29	57.65	16.18	7.87	0.96	1.26	3.55	188	196	143	154	440	73	111
D 61	5.6	59.06	17.01	7.02	1.03	1.23	3.85	161	208	147	168	408	72	84
D 64	8.18	57.94	17.86	8.06	1.12	2.41	3.97	367	181	187	175	440	75	133
D 66	23.67	43.16	14.14	8.19	0.73	2.71	3.18	335	193	91	149	379	83	88
D 67	27.64	34.62	10.94	6.01	0.55	1.91	2.42	133	146	65	107	284	43	78

Sample	Zn	Mo	Y	Cr/V	Cr/Ni	SiO_2/Al_2O_3	Al_2O_3/TiO_2	$100*Fe_2O_3/Al_2O_3$	$100*TiO_2/Al_2O_3$	Ti/Zr	Zr/Ni	Zr/Cr
D 7	99	15	44	2.28	0	3.70	18.04	77.21	5.54	34.40	0	0.35
D 8	76	14	22	2.5	2.97	3.88	15.71	47.02	6.36	35.56	1.17	0.39
D 13	137	36	29	1.93	2.08	2.88	15.99	48.47	6.25	47.79	0.62	0.29
D 14	131	33	25	1.98	2.09	3.11	15.57	53.01	6.42	43.62	0.61	0.29
D 23	123	24	30	1.86	1.47	3.06	16.88	54.54	5.92	39.22	0.51	0.34
D 24	138	25	35	2.17	2.11	3.10	16.21	52.07	6.16	39.49	0.75	0.35
D 27	115	21	31	2.44	1.84	3.37	16.33	58.98	6.12	38	0.6	0.32
D 32	135	27	37	2.28	1.96	3.22	16.33	51.97	6.12	28.67	0.77	0.39
D 39	45	13	28	9.55	8.09	5.46	14.04	64.64	7.11	13.15	2.83	0.34
D 41	93	20	26	1.85	2.96	4.15	16.75	45.92	5.96	32.51	1.35	0.45
D 46	83	21	26	2.99	1.53	3.70	16.93	53.62	5.9	33.37	0.59	0.39
D 47	117	19	30	2.11	1.87	3.27	16.97	52.76	5.88	36.97	0.69	0.37
D 50	119	23	28	2.49	2.23	3.67	16.27	44.94	6.14	34.51	0.77	0.34
D 53	127	27	30	2.54	1.95	3.30	16.43	41.80	6.08	40.02	0.57	0.29
D 58	73	16	19	4.48	0	5.37	20.97	66.40	4.76	25.21	0	0.29
D 59	111	21	27	2.24	2.34	3.56	16.85	48.64	5.93	40.26	0.76	0.32
D 61	84	17	23	1.96	2.53	3.47	16.51	41.26	6.05	42.23	0.91	0.35
D 64	133	24	30	2.43	1.19	3.24	15.94	45.12	6.27	35.76	0.5	0.42
D 66	88	29	30	1.96	1.13	3.05	19.36	57.92	5.16	47.79	0.27	0.24
D 67	78	14	19	1.94	2.13	3.16	19.89	54.93	5.02	50.57	0.48	0.22

The basin was influenced by the uplift of the accretionary prism, which served as major contributor of sediment into the southern basin margin. Consistent with previous interpretations (e.g. Görür and Okay 1996; Elmas 2003), this forearc interpretation is also supported by numerous recent studies conducted on different portions of the basin, within both Hellenic and Turkish domains (e.g. Zattin et al. 2005; Tranos 2009; Sen and Yillar 2009; Islamoglu et al. 2010; Maravelis and Zelilidis 2010; Black et al. 2013; Görür and Elbek 2013; Maravelis and Zelilidis 2013; Tranos and Lacombe 2014).

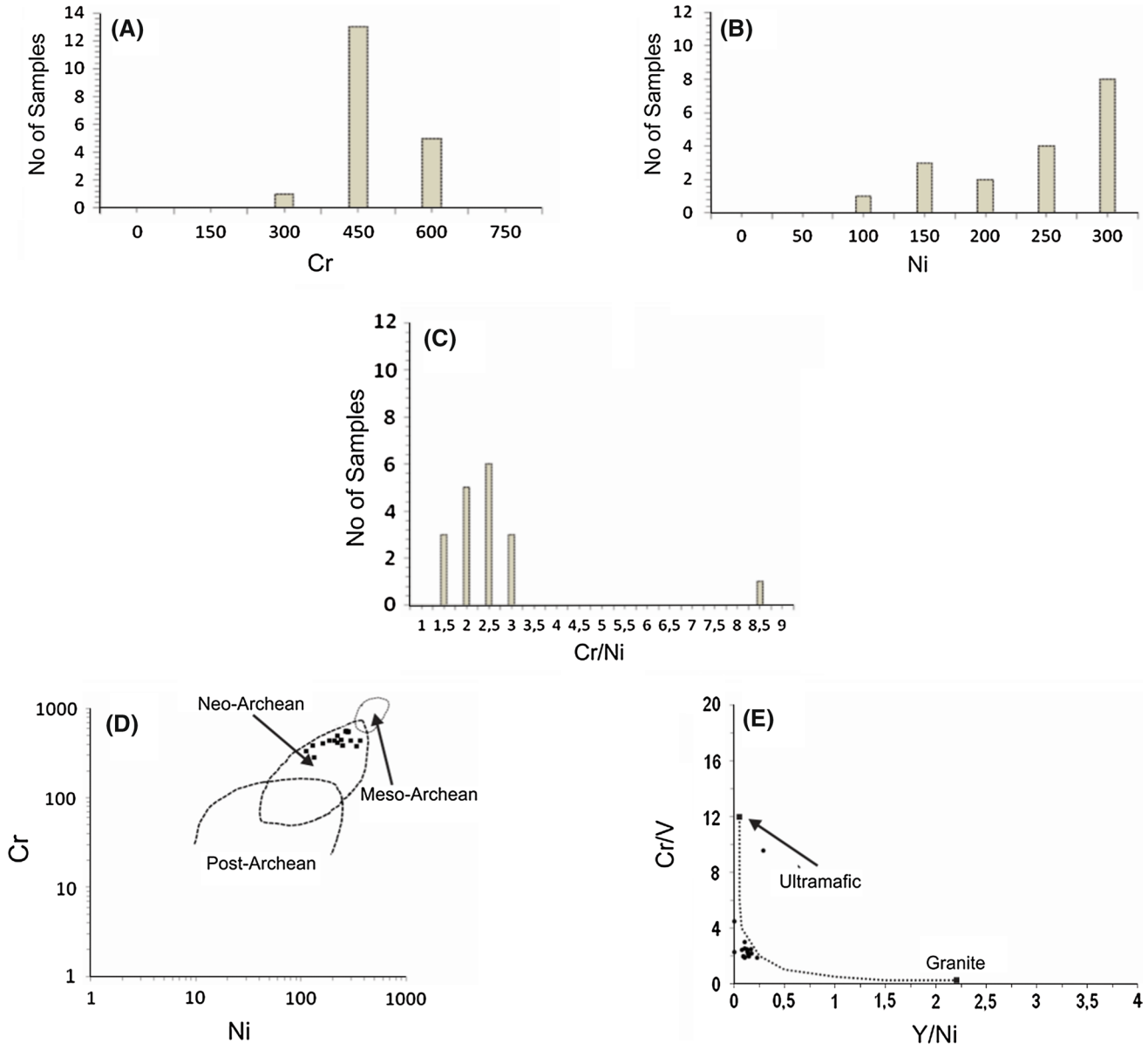

Fig. 11 Histograms, ratios, and chemical classification diagrams from the shallow-marine facies of the southern Thrace Basin (Lemnos Island). **a** Cr content. **b** Ni content. **c** Cr/Ni ratio (**a**, **b**, and **c** are from Garver et al. 1996). **d** Cr versus Ni (after Taylor and McLennan 1985). **e** Cr/V versus Y/Ni (after Hiscott 1984). The Cr/V versus Y/Ni diagram illustrates the importance of ophiolitic provenance. Ultramafic sources have very low Y/Ni and high Cr/V ratios. Mafic sources are with low Y/Ni ratio and high to moderate Cr/V ratios. All plots indicate mostly a mafic influence

An alternative interpretation suggests that the sedimentary assemblages on the southern Thrace (Lemnos Island) were derived from terranes of the north (Caracciolo et al. 2011), but this model provides no field evidence to support the Rhodopian influence (Maravelis and Zelilidis 2013). Although most forearc basin fills are derived chiefly from an attendant volcanic arc, in Thrace Basin, such influence is of minor importance in the southern basin margin. Instead, an accretionary prism source is indicated by: (1) the arcward palaeoflow pattern, (2) landward migration of the basin depocentre towards the magmatic arc, and (3) the abundance of mafic source rocks. The Thrace Basin is therefore one of the best examples of a mature, two-sided forearc basin succession with significant sediment input from a trenchward prism.

Provenance

The Cenozoic sedimentary successions in the Thrace Basin lie unconformably over different basement types, which

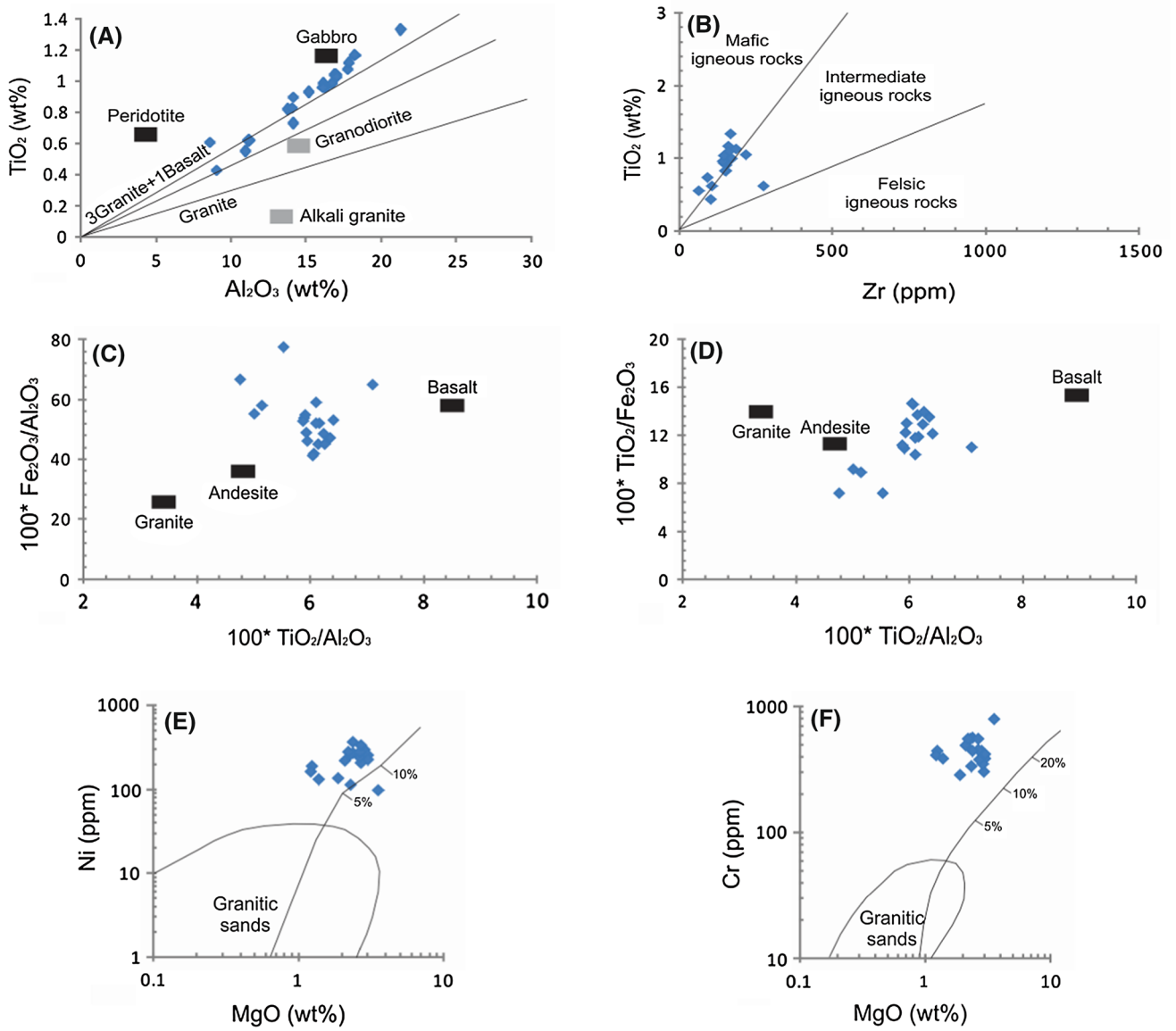

Fig. 12 Provenance discrimination diagrams from the studied sediments (Lemnos Island). **a** TiO_2 versus Al_2O_3 (after McLennan et al. 1980). The "granite" and "3 granite + 1 basalt" lines from Schieber (1992). **b** TiO_2 versus Zr (after Hayashi et al. 1997). **c** Fe_2O_3/Al_2O_3 versus TiO_2/Al_2O_3. **d** TiO_2/Fe_2O_3 versus TiO_2/Al_2O_3 (**c** and **d** are from Nesbitt and Wilson 1992). **e** Cr versus MgO. **f** Ni versus MgO (**e** and **f** are from Van de Kamp and Leake 1995 and Zhang 2004)

are separated by the NAF (Siyako and Huvaz 2007). In the north, the Eocene–Oligocene clastic deposits of the Thrace Basin overlie the metamorphic rocks of the Rhodope, whereas in the south they are underlain by ophiolitic and metamorphic rocks (Elmas 2011). The geochemical signature of the mudstone samples from the southern Thrace Basin reflects a mafic source terrane, typical of active tectonic settings. Mudstone-normalized REE values exhibit a pronounced LREE depletion indicating a fore-arc origin, and the minor positive Eu anomalies suggest accumulation in an active setting typified by the influx of juvenile mafic material (Maravelis and Zelilidis 2010). The sandstone lithic fragments suggest that mafic/ultramafic rocks and associated metamorphic rocks and sedimentary carapace served as the main sediment source for the studied deposits. Glaucophane suggests a provenance consisted of blueschist facies metamorphic source rock (an exhumed accretionary prism). Rare presence of neovolcanic lithic grains (Caracciolo et al. 2011) may represent a minor arc-derived component from the northern sources (Maravelis and Zelilidis 2010).

The southern Thrace Basin, in Hellenic and Turkish domains, contains granule to boulder conglomerates that form beds up to 5 m thick (Maravelis et al. 2007; Okay

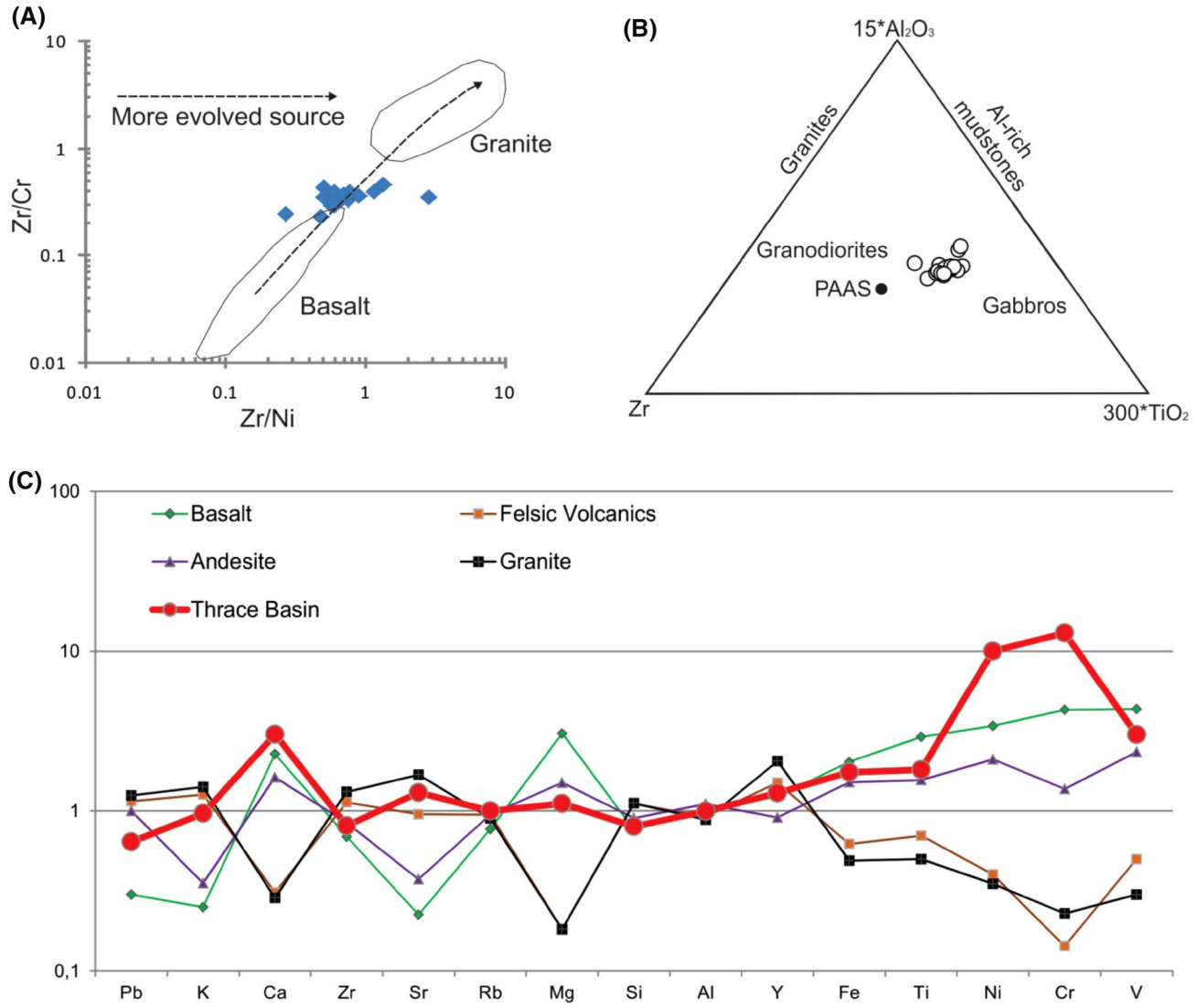

Fig. 13 Chemical classification diagram, ternary plot, and spider diagram from the southern Thrace Basin (Lemnos Island). **a** Zr/Cr versus Zr/Ni (from Hiscott 1984). **b** 15*Al_2O_3–300*TiO_2–Zr (from Garcia et al. 1991). **c** UCC-normalized spider diagram. The normalized element concentrations of granite, felsic volcanics, andesite, and basalt are also plotted for comparison (Condie 1993). UCC average is from Taylor and McLennan (1985). Elements are arranged from left to right in order of increasing normalized abundance in Mesozoic–Cenozoic (Condie 1993)

et al. 2010). Conglomerate types, seen in the deep-sea fans, range from unstratified poorly sorted pebble to cobble conglomerate with dispersed larger boulders, through well-organized clast-supported pebble to cobble conglomerate with sandstone, to beds of sandstone with granules and rare pebbles (Maravelis et al. 2007). Most conglomerates are ungraded, grading is seen near the base or near the top in some instances whereas, reverse grading occur in a number of beds (Maravelis 2009). The main rock types observed within the conglomerates are: (1) igneous rocks clasts of mafic and ultramafic composition, (2) low-grade metamorphic rock fragments, and (3) sedimentary rocks (Maravelis et al. 2007; Maravelis and Zelilidis 2010). In particular, these deposits contain chert, peridotite, schist, and igneous fragments, such as basalts and gabbros in addition to sandstone and limestone clasts (Maravelis et al. 2007; Okay et al. 2010). The results presented in this investigation suggest that the conglomerates in the overlying shallow-marine facies are composed of clasts of similar composition. The dominance of mafic and ultramafic igneous rocks, cherts and metamorphic rock fragments in association with the absence of felsic volcanics, makes the Rhodopian volcanic arc an unlikely source of the sediments. Potential source-area candidates are the Axios or sub-Pelagonian zones and the chert rock fragments in the conglomerates suggest that the latter is the most likely candidate.

All data suggest that metamorphic, sedimentary, and igneous rocks in a recycled orogenic environment were the most important source rocks. This is related to an accretionary prism provenance and indicates that the Thrace Basin is an example of a forearc basin that developed under the active influence of a nearby accretionary prism (Pindic Cordillera and/or Biga Peninsula).

Basin tectonics

The northward subduction of the African oceanic lithosphere beneath the Eurasian continental plate was the driving mechanism for the development of the active continental margin on the southeastern Balkan Peninsula (Fytikas et al. 1984; Le Pichon et al. 1995; Marchev et al. 2004; Maravelis and Zelilidis 2010; D'Atri et al. 2012). The subduction during the closure of a branch of the Neo-Tethyan Ocean formed the Rhodopian volcanic arc, the Thrace forearc basin, and the accretionary prism, which is exposed in northeast Greece (Pindic Cordillera) and northwest Turkey (Biga Peninsula) (Tranos 2009; Maravelis and Zelilidis 2010; D'Atri et al. 2012; Görür and Elbek 2013). Data from blueschist facies suggest active subduction and accretionary crustal growth associated with trenchward decrease in the degree of metamorphism from ultrahigh-pressure conditions in the Rhodope to blueschist–eclogite facies on Biga Peninsula (Topuz et al. 2008). During late Eocene time, this blueschist facies basement was partly exhumed and was enveloped by upper Eocene radiolarian chert, while its post-Miocene exhumation took place along a transpressional segment of the NAF (Topuz et al. 2008).

Late Cenozoic plutonic rocks in the North Aegean Sea result from subduction migration along the Hellenic Arc (Fytikas et al. 1984; Yilmaz et al. 2001). Their late Eocene–early Oligocene ages correspond to the late stages of subduction, whereas their late Oligocene–late Miocene ages indicate regional extension and exhumation (Black et al. 2013; Görür and Elbek 2013; Maravelis and Zelilidis 2013). Zircon ages indicate that the plutonic rocks on Biga Peninsula derived from different magma injections, with their late Eocene–early Oligocene ages recording the initial crystallization of magmas generated above the subducting slab (Black et al. 2013). Late Oligocene to Miocene ages document continued crystallization during exhumation related to the subduction slab roll-back along the Hellenic trench (McKenzie 1978; Bonev and Beccaletto 2007). Geochronologic studies indicate that exhumation was active during the early Miocene time (Cavazza et al. 2009).

The late orogenic processes in the broader area of Thrace Basin were related either to extension (Caracciolo et al. 2011; Cavazza et al. 2009) or a more complicated pattern of transpression to transtension regimes (Tranos 2009, Tranos and Lacombe 2014). U–Pb geochronology of plutonic rocks suggests regional subduction and suturing during late Eocene time, followed by late Oligocene to Miocene extension and exhumation of the plutons (Black et al. 2013). Additional evidence for this Late Paleogene exhumation event comes from metamorphic core complexes exhumed along the regional detachment faults from late Oligocene to the Miocene (Cavazza et al. 2009; Okay and Satır 2000). Tranos (2009) documented that during late Oligocene time, a NNW-SSE to N–S compression resulted in E–W to ENE–WSW open buckle folds and intense reverse faulting on the late Eocene to early Oligocene submarine fans. Structural analysis reveals a folding event characterized by open to gentle, slightly asymmetric buckle folds with interlimb angles of about 140°. The average fold axis plunges towards the WSW at subhorizontal to shallow (~11°) angles (Tranos 2009). This folding event indicates a regional NNW-SSE contraction that occurred during the Oligocene and before the early Miocene as it does not affect the lower Miocene volcanics (Tranos 2009; Maravelis and Zelilidis 2010). Age-equivalent compression has been reported within the eastern parts of the basin, in the Turkish domain (Görür and Okay 1996; Elmas 2012), and also in the Hellenic eastern Rhodope area (Koukouvelas and Doutsos 1990; Karfakis and Doutsos 1995; Tranos et al. 2009). Seismic stratigraphic data suggest that the bulk of the shortening was due to thin-skinned thrusting and folding that occurred from the base Paleocene to Eocene, with subsequent doming of overthrust tips in Oligocene time (Sinclair et al. 1997).

Typical forearc basins are characterized by the deposition of thick successions of submarine fans at the expense of shallower marine sediments (Trop and Ridgway 2007; Fildani et al. 2008; Mitchell et al. 2010; Maravelis and Zelilidis 2013). The southern edge of the Thrace Basin, within both the Hellenic and Turkish domains, is mainly dominated by deep-marine strata with a shoaling upward trend into shallow-marine and non-marine strata observed at the top of the succession. Because global eustatic sea-level fluctuations were negligible during this time (Miller et al. 2011), the regional shoaling upward trend requires tectonically driven uplift (Maravelis and Zelilidis 2010). The driving force behind this uplift is most likely related to uplift of the accretionary prism (Fig. 14). The late Eocene–early Oligocene basin fill consists of two intervals: (1) a lower, 500–1000 m sand-rich submarine-fan system, and (2) an upper, 100–150-m-thick shallow-marine to deltaic sedimentary unit (Lalechos 1986; Perinçek 1991; Turgut et al. 1991; Roussos 1994; Turgut and Eseller 2000; Maravelis et al. 2007; Maravelis and Zelilidis 2011; D'Atri et al. 2012). Subduction tectonics affected the palaeogeography and gravity-flow deposits migrated northeastward against the continental slope. These flows, largely turbidity currents, accumulated widespread, thick, sand-rich sediments.

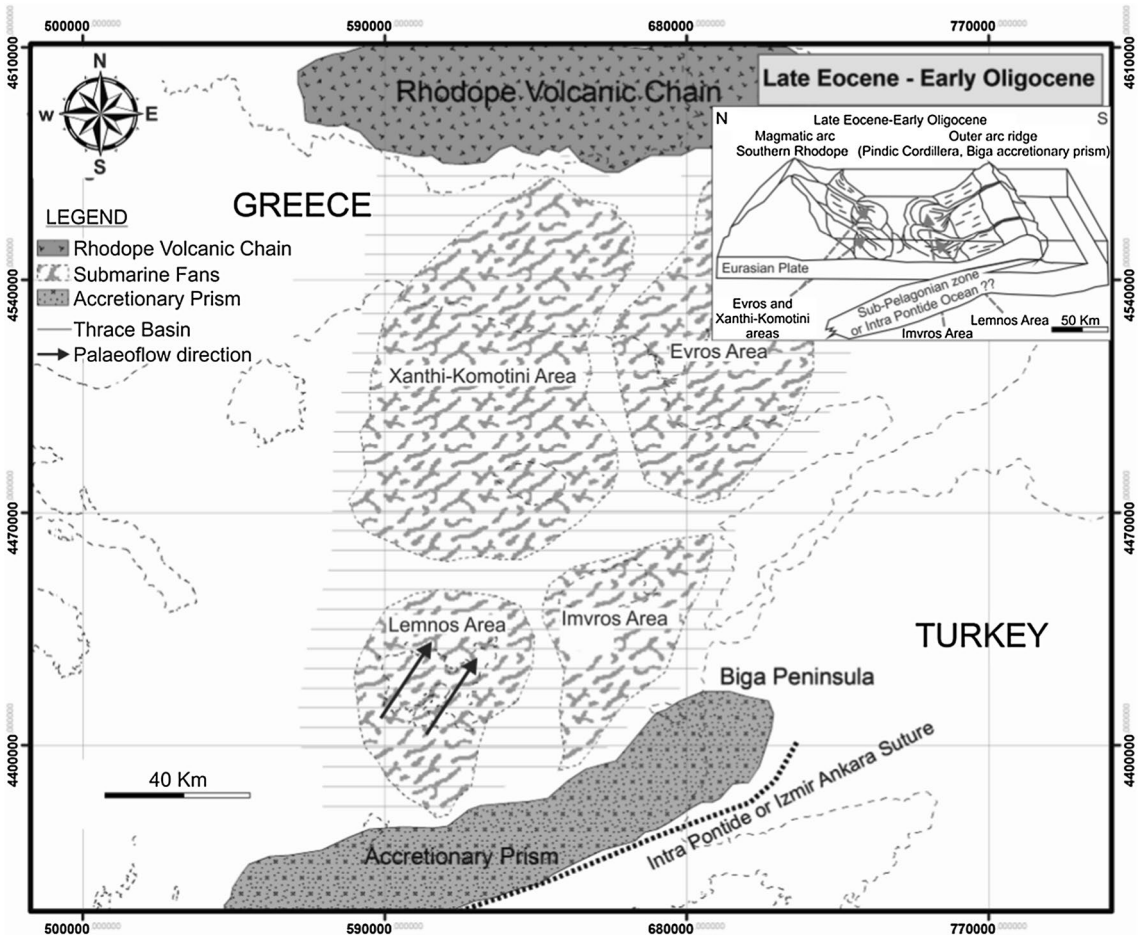

Fig. 14 Paleotectonic cross section that depicts the regional plate tectonic configuration (from Maravelis and Zelilidis 2010). Palaeogeographic map illustrating the depositional setting of Thrace Basin. The basin fill records the exhumation of a coeval accretionary prism (Pindic Cordillera and Biga Peninsula). This uplift leads to a two-sided forearc basin succession with significant sediment input from the trenchward prism. Both arcward- and trenchward-derived sediment forms submarine-fan systems that fill the basin depocentres

Uplift of the accretionary prism shifted the locus of coarse-grained sedimentation landwards, towards the magmatic arc. Once subaerially exposed, this prism contributed sediment northeastwards towards the magmatic arc (Maravelis and Zelilidis 2013). The submarine-fan system prograded towards the NE-NNE, as evident by the overlap of the inner fan above the outer fan (Turgut et al. 1991; Maravelis et al. 2007; Maravelis 2009; Maravelis and Zelilidis 2010; 2011; D'Atri et al. 2012). On southern Thrace Basin, extensive palaeocurrent analysis performed on submarine fans on both Hellenic and Turkish domains revealed a NE-NNE-ward flow, making the northern Rhodopian magmatic belt an unlikely source of sediment (Perinçek 1991; Turgut et al. 1991; Maravelis et al. 2007; Maravelis 2009). Palaeoflow results presented in this study also indicate a dominant NE-NNE-ward palaeoflow direction. Palaeomagnetic studies show no rotation of the eastern Rhodope–Thrace region from the Oligocene onwards and imply that the NE-NNE palaeocurrent pattern was the primary direction (Kissel and Laj 1988). Kondopoulou (2000) suggested a c. 25° clockwise rotation since 17 Ma for the Lemnos Island. If it is correct, an S–N palaeoflow direction is indicated, documenting the influence of the southern accretionary prism.

The tectonically driven uplift of the accretionary prism and its influence on forearc basins has been documented in similar ancient settings such as, in the Maastrichtian Great Valley Basin, California (Mitchell et al. 2010). In Great Valley Basin, the accretion of oceanic crust and sediment to the upper plate caused the growth of an accretionary prism. Structural uplift and emergence is documented from fanning of seismic reflector dips that is consistent with syntectonic growth strata. Following this emergence, prograding submarine fans and shelf deposits filled the basin from north to south. This progradational package marked the onset of a shoaling upward trend within the basin. The importance of accretionary prism growth into forearc

settings can also be observed in the modern forearc basins of Peru and Chile (Laursen and Normark 2003), the Philippines (Hayes and Lewis 1984), Indonesia (Matson and Moore 1992), and Alaska (Dobson et al. 1991). All of these profiles show the importance of progressive arcward onlap as well as angularities within the basin fill created by progressive arcward folding and tilting of the basin due to accretionary prism growth. In particular along the Sunda arc–trench system of Indonesia, several islands represent an emergent outer arc (e.g. Nias). Erosion of these islands feeds an arcward prograding system. In particular, the Nias delta systems have constructed a coastal plain extending 15 km from the centre of the island. From the coastline, the shelf and slope have prograded another 15 km into the forearc trough.

Conclusions

The lower Oligocene shallow-marine facies in the southern margin of the Hellenic Thrace Basin (Lemnos Island) offers insights into active convergent margins. Integration of sedimentological, stratigraphic, palaeocurrent, and provenance investigations indicate a direct relationship between sedimentary packaging and regional tectonics. During late Eocene to early Oligocene, the basin served as a forearc basin with significant sediment input from a nearby, southern positioned, accretionary prism (e.g. Pindic cordillera and/or Biga Peninsula).

The shallow-marine sediments correspond to the upslope evolution of a regional well-studied upper Eocene to lower Oligocene sand-rich submarine-fan system. This system is exposed on both Turkish and Hellenic domains and forms part of the larger number of fan systems that filled the southern part of the basin. With respect to the underlying deep-sea sediments, the studied rocks are typified by the same: (1) NE-NNE palaeodispersal direction, towards the toe of the Rhodopian magmatic arc, (2) landward migration of the basin depocentre, (3) no evidence of structural deformation involving normal faulting, (4) sedimentary petrography data that suggest an oceanic origin, (5) geochemical values that reflect a mafic source terrane, and (5) conglomerate clast composition that is most likely derived from the accretionary prism.

These data indicate consistent influence of the accretionary prism into the basin fill, as the accretionary prism underwent tectonically driven uplift and compression.

Acknowledgments The work presented in this article represents internally funded research conducted by the authors as part of the Department of Geology, University of Patras, Greece. The authors gratefully thank StratoChem Laboratories, Cairo, Egypt, for the geochemical analysis. The authors acknowledge the journal editor Prof. Wolf-Christian Dullo, and the journal reviewers Jeffrey M. Trop, Markos Tranos, and Kathleen Surpless for their constructive discussions and thorough editing that largely improved the manuscript.

References

Amorosi A, Colalongo ML, Dinelli E, Lucchini F, Vaiani SC (2007) Cyclic variations in sediment provenance from late Pleistocene deposits of the eastern Po Plain, Italy. Geol Soc Am Spec Pap 420:13–24

Beccaletto L, Bartolini AC, Martini R, Hochuli PA, Kozur H (2005) Biostratigraphic data from the Çetmi Melange, northwest Turkey: palaeogeographic and tectonic implications. Palaeogeo Paleocl 221:215–244

Berglar K, Gaedicke C, Lutz R, Franke D, Djajadihardja YS (2008) Neogene subsidence and stratigraphy of the Simeule forearc basin. Mar Geol 253:1–13

Black KN, Catlos EJ, Oyman T, Demirbilek M (2013) Timing Aegean extension: evidence from in situ U–Pb geochronology and cathodoluminescence imaging of granitoids from NW Turkey. Lithos 180–181:92–108

Bonev N, Beccaletto L (2007) From syn- to post-orogenic tertiary extension in the north Aegean region: constraints on the kinematics in the eastern Rhodope-Thrace, Bulgaria-Greece and the Biga Peninsula, NW Turkey. Geol Soc Lond Spec Pub 291:113–142

Bowman AP, Johnson HD (2013) Storm-dominated shelf-edge delta successions in a high accommodation setting: the palaeo-Orinoco Delta (Mayaro Formation), Columbus Basin, South-East Trinidad. Sedimentology. doi:10.1111/sed.12080

Bradshaw JD, Vaughan APM, Millar IL, Flowerdew MJ, Trouw RAJ, Fanning CM, Whitehouse MJ (2012) Permo-Carboniferous conglomerates in the Trinity Peninsula Group at View Point, Antarctic Peninsula: sedimentology, geochronology and isotope evidence for provenance and tectonic setting in Gondwana. Geol Mag 149:626–644

Caracciolo L, Critelli S, Innocenti F, Kolios N, Manetti P (2011) Unraveling provenance from Eocene–Oligocene sandstones of the Thrace Basin, North-east Greece. Sedimentology 58:1988–2011

Catuneanu O, Abreu V, Bhattacharya JP, Blum MD, Dalrymple RW, Eriksson PG, Fielding CR, Fisher WL, Galloway WE, Gibling MR, Giles KA, Holbrook JM, Jordan R, Kendall CGSC, Macurda B, Martinsen OJ, Miall AD, Neal JE, Nummedal D, Pomar L, Posamentier HW, Pratt BR, Sarg JF, Shanley KW, Steel RJ, Strasser A, Tucker ME, Winker C (2009) Towards the standardization of sequence stratigraphy. Earth Sci Rev 92:1–33

Catuneanu O, Galloway WE, Kendall CGSC, Miall AD, Posamentier HW, Strasser A, Tucker ME (2011) Sequence stratigraphy: methodology and nomenclature. Newslett Stratigr 44:173–245

Cavazza W, Okay AI, Zattin M (2009) Rapid early-middle Miocene exhumation of the Kazdağ Massif (western Anatolia). Int J Earth Sci 98:1935–1947

Cingolani CA, Manassero M, Abre P (2003) Composition, provenance and tectonic setting of Ordovician siliciclastic rocks in the San Rafael Block: southern extension of the Precordillera crustal fragment, Argentina. J South Am Earth Sci Rev 16:91–106

Clift PD, Pavlis T, DeBari S, Draut A, Rioux M, Kelemen P (2005) Subduction erosion of the Jurassic Talkeetna–Bonanza arc and the Mesozoic accretionary tectonics of western North America. Geology 33:881–884

Condie KC (1993) Chemical composition and evolution of the upper continental crust: contrasting results from surface samples and shales. Chem Geol 104:1–37

Cullers RL (2000) The geochemistry of shales, siltstones and sandstones of Pennsylvanian-Permian age, Colorado, USA: implications for provenance and metamorphic studies. Lithos 51:181–203

D'Atri A, Zuffa GG, Cavazza W, Okay AI, Di Vincenzo G (2012) Detrital supply from subduction/accretion complexes to the Eocene–Oligocene postcollisional southern Thrace Basin (NW Turkey and NE Greece). Sediment Geol 243–244:117–129

De Gasperi A, Catuneanu O (2014) Sequence stratigraphy of the Eocene turbidite reservoirs in the Albacora field, Campos Basin, offshore Brazil. AAPG Bull 98:279–313

DeGraaff-Surpless K, Graham SA, Wooden JL, Mc Williams MO (2002) Detrital zircon provenance analysis of the Great Valley Group, California: evolution of an arc–forearc system. Geol Soc Am Bull 114:1564–1580

Dewey JF, Sengör AMC (1979) Aegean and surrounding regions: complex multiplate and continuum tectonics in a convergent zone. Geol Soc Am Bull 90:84–92

Dickinson WR, Seely DR (1979) Structure and stratigraphy of forearc regions. AAPG Bull 63:2–31

Dimitriadis S, Kondopoulou D, Atzemoglou A (1998) Dextral rotations and tectonomagmatic evolution of the southern Rhodope and adjacent regions (Greece). Tectonophysics 299:159–173

Dixon JF, Steel RJ, Olariu C (2012) River-dominated, shelf-edge deltas: delivery of sand across the shelf break in the absence of slope incision. Sedimentology 59:1133–1157

Dobson MR, Scholl DW, Stevenson AJ (1991) Interplay between arc tectonics and sea-level changes as revealed by sedimentation patterns in the Aleutians. In: Macdonald DIM (ed) Sedimentation, tectonics and eustacy: sea-level changes at active margins. Oxford, Special Publication 12, pp 151–163

Elmas A (2003) Late Cenozoic tectonics and stratigraphy of northwestern Anatolia: the effects of the North Anatolian fault to the region. Int J Earth Sci 92:380–396

Elmas A (2011) The Thrace Basin: stratigraphic and tectonicpalaeogeographic evolution of the Palaeogene formations of northwest Turkey. Int Geol Rev 54:1419–1442

Elmas A (2012) Basement types of the Thrace Basin and a new approach to the pre-Eocene tectonic evolution of the northeastern Aegean and northwestern Anatolia: a review of data and concepts. Int J Earth Sci 101:1895–1911

Fildani A, Hessler AM, Graham SA (2008) Trench–forearc interactions reflected in the sedimentary fill of Talara basin, northwest Peru. Basin Res 20:305–331

Finzel ES, Trop JM, Ridgway KD, Enkelmann E (2011) Upper plate proxies for flat-slab subduction processes in southern Alaska. Earth Planet Sci Lett 3:348–360

Fytikas M, Innocenti F, Manetti P, Mazzuoli R, Peccerillo A, Villari L (1984) Tertiary to quaternary evolution of the volcanism in the Aegean Region. In: Dixon JE, Robertson AHF (eds) The geological evolution of the Eastern Mediterranean. Geological Society of London Special Publication, pp 687–699

Gao S, Wedepohl KH (1995) The negative Eu anomaly in Archean sedimentary rocks: implication for decomposition, age and importance of their granitic sources. Earth Planet Sci Lett 133:81–94

Garcia D, Coehlo J, Perrin M (1991) Fractionation between TiO2 and Zr as a measure of sorting within shale and sandstone series (northern Portugal). Eur J Mineral 3:401–414

Garver JI, Royce PR, Smick TA (1996) Chromium and nickel in shale of the Taconic foreland: a case study for the provenance of fine-grained sediments with an ultramafic source. J Sediment Res 66:100–106

Görür N, Elbek S (2013) Tectonic events responsible for shaping the Sea of Marmara and its surrounding region. Geodin Acta. doi:10.1080/09853111.2013.859346

Görür N, Okay A (1996) A fore-arc origin for the Thrace Basin, NW Turkey. Int J Earth Sci 85:662–668

Hayashi K, Fujisawa H, Holland H, Ohmoto H (1997) Geochemistry of ~ 1.9 Ga sedimentary rocks from northeastern Labrador, Canada. Geochim Cosmochim Acta 61(19):4115–4137

Hayes DE, Lewis SD (1984) A geophysical study of the Manila trench, Luzon, Philippines: crustal structure, gravity, and regional tectonic evolution. J Geophys Res 89:9171–9195

Hessler AM, Lowe DR (2006) Weathering and sediment generation in the Archean: an integrated study of the evolution of siliciclastic sedimentary rocks of the 3.2 Ga Moodies Group, Barberton Greenstone Belt, South Africa. Precambrian Res 151:185–210

Hiscott RN (1984) Ophiolitic source rocks for Taconic-age flysch: trace-element evidence. Geol Soc Am Bull 95:1261–1267

Hubert-Ferrari A, Armijo R, King G, Meyer B, Barka A (2002) Morphology, displacement, and slip rates along the North Anatolian Fault, Turkey. J Geophys Res 107:ETG 9-1–ETG 9-33

Ingersoll RV (1983) Petrofacies and provenance of Late Mesozoic forearc basin, Northern and Central California. AAPG Bull 67:1125–1142

Innocenti F, Manetti P, Mazzuoli R, Pertusati P, Fytikas M, Kolios N (1994) The geology and geodynamic significance of the island of Limnos, North Aegean Sea, Greece. Neues Jahrb Geol Paläontol 11:661–691

Islamoğlu Y, Harzhauser M, Gross M, Jiménez-Moreno G, Coric S, Kroh A, Rögl F, van der Made J (2010) From Tethys to Eastern Paratethys: oligocene depositional environments, paleoecology and paleobiogeography of the Thrace Basin (NW Turkey). Int J Earth Sc 99:83–200

Karfakis I, Doutsos T (1995) Late orogenic evolution of the Circum–Rhodope Belt, Greece. Neues Jahrb Geol P-A5:305–319

Kissel C, Laj C (1988) The tertiary geodynamical evolution of the Aegean arc: a paleomagnetic reconstruction. Tectonophysics 146:183–201

Kneller B (1995) Beyond the turbidite paradigm: physical models for deposition of turbidites and their implications for reservoir prediction. In: AJ Hartley, DJ Prosser (eds) Characterisation of Deep Marine Clastic Systems. Geological Society London Special Publication 94, pp 31–49

Kochelek EJ, Amato JM, Pavlis TL, Clift PD (2011) Flysch deposition and preservation of coherent bedding in an accretionary complex: detrital zircon ages from the Upper Cretaceous Valdez Group, Chugach terrane, Alaska. Lithosphere 3:265–274

Kondopoulou D (2000) Palaeomagnetism in Greece: Cenozoic and Mesozoic components and their geodynamic implications. Tectonophysics 326:131–151

Konstantopoulos P, Zelilidis A (2013) Provenance analysis of Eocene–Oligocene turbidite deposits in Pindos Foreland Basin, fold and thrust belt of SW Greece: constraints from framework petrography and bulk-rock geochemistry. Arab J Geosci 6:4671–4700

Kortyna C, Trop JM, Idleman B (2013) Integrated provenance record of a forearc basin modified by slab window magmatism: detrital zircon geochronology and sandstone compositions of the Paleogene Arkose Ridge Formation, south central Alaska. Basin Res 25:1–25

Koukouvelas I, Doutsos T (1990) Tectonic stages along a traverse cross cutting the Rhodopian zone (Greece). Int J Earth Sci 79:753–776

Lalechos N (1986) Correlations and observations in molassic sediments in onshore and offshore areas of Northern Greece. Mineral Wealth 42:7–34

Laursen J, Normark WR (2003) Impact of structural and autocyclic basin-floor topography on the depositional evolution of the deep-water Valparaiso forearc basin, central Chile. Basin Res 15:201–226

Le Pichon X, Chamot-Rooke N, Lallemant SL, Noomen R, Veis G (1995) Geodetic determination of kinematics of Central Greece with respect to Europe: implications for eastern Mediterranean tectonics. J Geophys Res 100:12675–12690

Lonergan L, Lee N, Johnson HD, Cartwright JA, Jolly RJH (2000) Remobilization in deepwater depositional systems: implications for reservoir architecture and prediction. In: Weimer P, Slatt RM, Coleman J, Rosen NC, Nelson H, Bouma AR, Styzen MJ, Lawrence DT (eds) Deep water reservoirs of the world, GCSSEPM Foundation 20th Annual Bob F Perkins Research Conference, pp 515–531

Lowe DR (1982) Sediment gravity flows II: depositional models with special reference to the deposits of high density turbidity currents. J Sediment Petrol 52:279–297

Maravelis A (2009) Provenance, tectonic setting and source rock potential of the Paleogene deep-water sediments on Lemnos Island Northeast Greece. Implications of the Northeast Aegean Sea hydrocarbon potential and configuration. Dissertation, University of Patras, 287 pp

Maravelis A, Zelilidis A (2010) Petrography and geochemistry of the late Eocene–early Oligocene submarine fans and shelf deposits on Lemnos Island, NE Greece: implications for provenance and tectonic setting. Geol J 45:412–433

Maravelis A, Zelilidis A (2011) Geometry and sequence stratigraphy of the Late Eocene–Early Oligocene shelf and basin floor to slope turbidite systems, Lemnos Island, NE Greece. Stratigr Geol Correl 19:205–220

Maravelis A, Zelilidis A (2012) Paleoclimatology and Paleoecology across the Eocene/Oligocene boundary, Thrace Basin, Northeast Aegean Sea, Greece. Palaeogeogr Palaeocl 365–366:81–98

Maravelis A, Zelilidis A (2013) Discussion: "Unraveling the provenance of Eocene–Oligocene sandstones of the Thrace Basin, North-east Greece" by Caracciolo et al. (2011) Sedimentology 58:1988–2011. Sedimentology 60:860–864

Maravelis A, Konstantopoulos P, Pantopoulos G, Zelilidis A (2007) North Aegean sedimentary basin evolution during the late Eocene to early Oligocene based on sedimentological studies on Lemnos Island (NE Greece). Geol Carpath 58:455–464

Marcaillou B, Collot JY (2008) Chronostratigraphy and tectonic deformation of the North Ecuadorian–South Colombian offshore Manglares forearc basin. Mar Geol 255:30–44

Marchev P, Raicheva R, Downes H, Vaselli O, Chiaradia M, Morit R (2004) Compositional diversity of Eocene–Oligocene basaltic magmatism in the Eastern Rhodopes, SE Bulgaria: implications for genesis and tectonic setting. Tectonophysics 393:301–328

Matson RG, Moore GF (1992) Structural influences on Neogene subsidence in the central Sumatra forearc basin. In Walkins JS, Zhigiaj F, McMillen KJ (eds) Geology and geophysics of continental margins. Am Assoc Pet Geol Bull 53:157–181

McKenzie DP (1978) Some remarks on the development of sedimentary basins. Earth Planet Sci Lett 40:25–32

Mclennan SM, Nance WB, Taylor SR (1980) Rare earth element thorium correlations in sedimentary rocks and the composition of the continental crust. Geochim Cosmochim Acta 44:1833–1839

McLennan SM, Hemming S, McDaniel DK, Hanson GN (1993) Geochemical approaches to sedimentation, provenance and tectonics. In: Johnsson MJ, Basu A (eds) Processes controlling the composition of clastic sediments. Geological Society of America Special Paper, Boulder, Colorado vol 284, pp 21–40

Miller KG, Mountain GS, Wright JD, Browning JV (2011) A 180-million-year record of sea level and ice volume variations from continental margin and deep-sea isotopic records. Oceanography 24:40–53

Mitchell C, Graham SA, Suek DH (2010) Subduction complex uplift and exhumation and its influence on Maastrichtian forearc stratigraphy in the Great Valley Basin, northern San Joaquin Valley, California. Geol Soc Am Bull 122:2063–2078

Mountrakis D, (2006) Tertiary and Quaternary tectonics of Greece. In: Dilek Y, Pavlides S (eds.) Postcollisional tectonics and magmatism in the Mediterranean region and Asia. Geological Society of America Special Paper 409, pp 125–136

Mulder T, Alexander J (2001) The physical character of subaqueous sedimentary density flows and their deposits. Sedimentology 48:269–299

Nesbitt HW, Wilson RE (1992) Recent chemical weathering of basalts. Am J Sci 292:740–777

Okay AI, Satır M (2000) Coeval plutonism and metamorphism in a latest Oligocene metamorphic core complex in northwest Turkey. Geol Mag 137:495–516

Okay AI, Satir M, Zattin M, Cavazza W, Topuz G (2008) An Oligocene ductile strike-slip shear zone: the Uludağ Massif, northwest Turkey—implication for the westward translation of Anatolia. Geol Soc Am Bull 120:893–911

Okay AI, Ozcan E, Cavazza W, Okay N, Gyorgy L (2010) Basement types, Lower Eocene series, Upper Eocene Olistostromes and the initiation of the southern Thrace basin, NW Turkey. Turk J Earth Sci 19:1–25

Pantopoulos G, Zelilidis A (2012) Petrographic and geochemical characteristics of Paleogene turbidite deposits in the southern Aegean (Karpathos Island, SE Greece): implications for provenance and tectonic setting. Chem Erde Geochem 72:153–166

Paquet F, Proust JN, Barnes PM, Pettinga JR (2011) Controls on active forearc basin stratigraphy and sediment fluxes: the Pleistocene of Hawke Bay, New Zealand. Geol Soc Am Bull 123:1074

Pemberton GS, Spila M, Pulham AJ, Saunders T, MacEachern JA, Robbins D, Sinclair IK (2002) Ichnology and sedimentology of shallow marine to marginal marine systems: Ben Nevis and Avalon Reservoirs, Jeanne d'Arc Basin. Geol Assoc Canada Short Course Notes 15:343

Pe-Piper G, Piper DJW (2001) Late Cenozoic, post-collisional Aegean igneous rocks: Nd, Pb and Sr isotopic constraints on petrogenetic and tectonic models. Geol Mag 138:653–668

Pe-Piper G, Piper DJW, Koukouvelas I, Dolansky L, Kokkalas S (2009) Postorogenic shoshonitic rocks and their origin by melting underplated basalts: the Miocene of Limnos, Greece. Geol Soc Am Bull 121:39–54

Perinçek D (1991) Possible strand of the North Anatolian fault in the Thrace Basin, Turkey—an interpretation. AAPG Bull 75:241–257

Peytcheva I, Kostitsin Y, Salvikova E, Kamenov B, Klain L (1998) Rb–Sr and U–Pb isotope data for the Rila–West-Rhodopes batholith. Geochem Mineral Pet 35:93–105

Piper DJW, Normark WR (2009) Processes that initiate turbidity currents and their influence on turbidites: a marine geology perspective. J Sediment Res 79:347–362

Porebski SJ, Steel RJ (2003) Shelf-margin deltas: their stratigraphic significance and relationship to deepwater sands. Earth Sci Rev 62:283–326

Ridgway DR, Trop JM, Finzel ES (2012) Modification of continental forearc basins by flat-slab subduction processes: a case study from southern Alaska. In: Busby C, Azor A (eds) Tectonics of sedimentary basins: recent advances. Willey Blackwell, London, pp 327–346

Roser BP, Korsch RJ (1986) Determination of tectonic setting of sandstone–mudstone suites using SiO_2 content and K_2O/Na_2O ratio. J Geol 94:635–650

Roussos N (1994) Stratigraphy and palaeogeographical evolution of the Paleogene molassic basins of the N, Greece. Bull Geol Soc Greece 30:275–294

Schieber J (1992) A combined petrographical–geochemical provenance study of the newland formation, Mid-Proterozoic of Montana. Geol Mag 129:223–237

Şen S, Yıllar S (2009) The Korudağ anticlinorium in the south Thrace Basin, northwest Turkey: a super giant petroleum trap complex? AAPG Bull 93:357–377

Şengün F, Yiğitbaş E, Tunç IO (2011) Geology and tectonic emplacement of eclogite and blueschists, Biga Peninsula, northwest Turkey. Turk J Earth Sci 20:273–285

Sinclair HD, Juranov SG, Georgiev G, Byrne P, Mountrey NP (1997) The Balkan thrust wedge and foreland basin of Eastern Bulgaria: structural and stratigraphic development. In: AG Robertson (ed) Regional and petroleum geology of the Black Sea and surrounding region. AAPG Bull Memoir 68:91–114

Siyako M, Huvaz O (2007) Eocene stratigraphic evolution of the Thrace basin, Turkey. Sediment Geol 198:75–91

Spakman W, Wortel MJR, Vlaar NJ (1988) The Hellenic subduction zone: a tomographic image and its geodynamic implications. Geophys Res Lett 15:60–63

Talling PJ, Masson DG, Sumner EJ, Malgesini G (2012) Subaqueous sediment density flows: depositional processes and deposit types. Sedimentology 59:1937–2003

Tao H, Sun S, Wang Q, Yang X, Jiang L (2014) Petrography and geochemistry of Lower Carboniferous greywacke and mudstones in Northeast Junggar, China: implications for provenance, source weathering, and tectonic setting. J Asian Earth Sci 87:11–25

Taylor SR, McLennan SM (1985) The continental crust: its composition and evolution. Blackwell, Oxford 312

Topuz G, Okay AI, Altherr R, Satir M, Schwarz WH (2008) Late Cretaceous blueschist facies metamorphism in southern Thrace (Turkey) and its geodynamic implications. J Metamorph Geol 26:895–913

Tranos MD (2009) Faulting of Lemnos Island; a mirror of faulting of the North Aegean Trough (Northern Greece). Tectonophysics 467:72–88

Tranos DM, Lacombe O (2014) Late Cenozoic faulting in SW Bulgaria: fault geometry, kinematics and driving stress regimes. Implications for late orogenic processes in the Hellenic hinterland. J Geodyn 74:32–55

Tranos MD, Eleftheriadis GE, Kilias AA (2009) Philippi granitoid as a proxy for the Oligocene and Miocene crustal deformation in the Rhodope Massif (Eastern Macedonia, Greece). Geotecton Res 96:69–85

Trop JM (2008) Latest Cretaceous forearc basin development along an accretionary convergent margin: South-central Alaska. Geol Soc Am Bull 120:207–224. doi:10.1130/B26215.1

Trop JM, Ridgway KD (2007) Mesozoic and Cenozoic tectonic growth of southern Alaska: a sedimentary basin perspective. In: Ridgway KD, Trop JM, Glen JMG, O'Neill JM (eds) Tectonic growth of a collisional continental margin: crustal evolution of Southern Alaska. Geological Society of America Special Paper 431, pp 55–94

Turgut S, Eseller G (2000) Sequence stratigraphy, tectonics and depositional history in eastern Thrace Basin, NW Turkey. Mar Pet Geol 17:61–100

Turgut S, Türkaslan M, Perinçek D (1991) Evolution of the Thrace sedimentary basin and its hydrocarbon prospectivity. In: Spencer AM (ed) Generation, accumulation, and production of Europe's hydrocarbons. Eu Asso Pet Geosci Sp Pub, pp 415–437

Unruh JR, Dumitru TA, Sawyer TL (2007) Coupling of early tertiary extension in the Great Valley forearc basin with blueschist exhumation in the underlying Franciscan accretionary wedge at Mount Diablo, California. Geol Soc Am Bull 119:1347–1367

Van de Kamp PC, Leake BE (1995) Petrology and geochemistry of siliciclasic rocks of mixed feldspathic and ophiolitic provenance in the Northern Apennines, Italy. Chem Geol 122:1–20

Wang C, Li X, Liu Z, Li Y, Jansa L, Dai J, Wei Y (2012) Revision of the Cretaceous-Paleogene stratigraphic framework, facies architecture and provenance of the Xigaze forearc basin along the Yarlung Zangbo suture zone. Gondwana Res 22:415–433

Williams TA, Graham SA (2013) Controls on forearc basin architecture from seismic and sequence stratigraphy of the Upper Cretaceous Great Valley Group, central Sacramento Basin, California. Int Geol Rev 55:2030–2059

Yilmaz Y, Genç SC, Karacik Z, Altankaynak S (2001) Two contrasting magmatic associations of NW Anatolia and their tectonic significance. J Geodyn 31:243–271

Zattin M, Okay AI, Cavazza W (2005) Fission-track evidence for late Oligocene and mid-Miocene activity along the North Anatolian fault in south-western Thrace. Terra Nova 17:95–101

Zhang KJ (2004) Secular geochemical variations of the Lower Cretaceous siliciclastic rocks from central Tibet (China) indicate a tectonic transition from continental collision to back-arc rifting. Earth Planet Sci Lett 229:73–89